On Siegert pseudostates: formal concepts and s-wave illustrations in one- and two-channel central potentials

Abstract

Quantum scattering theory aims to model the interactions of particles in the quantum regime as the particles scatter from one another. The theoretical understanding of these events often necessitates solutions to the time-independent Schrödinger equation. For computational purposes, it becomes necessary to limit consideration of a scattering event to a finite volume of space. It is then crucial that the solutions to the time-independent Schrödinger equation obey a valid boundary condition at the boundary of the volume. In this study, solutions are forced to obey the Siegert boundary condition. The resulting wave functions are called Siegert pseudostates. Siegert pseudostates are a basis capable of representing physical scattering scenarios, including scenarios in which outgoing particle flux must escape the finite interaction volume. The application of the Siegert boundary condition eliminates the Hermiticity of the Hamiltonian, allowing for a complex eigenvalue, which results in an entirely discrete complex energy spectrum. Shape and Feshbach resonances are discussed and identified by the characteristically small imaginary part of their energy. A wave packet, serving as a model for a physical particle, is represented as a superposition of Siegert pseudostates, and allowed to evolve in time. Numerical investigations throughout the study validate the formalism.

Contents

I. Acknowledgments 3

II. Introduction 3

III. Formal concepts in one-channel 7

A. Derivation of Siegert pseudostates 7

B. k spectrum and E spectrum of a central square well 10

C. Shape resonance 11

D. Shape resonance in the Bain potential 15

E. Orthogonality and completeness 17

F. Numerical validation of completeness 27

G. Time evolution 30

H. Testing the accuracy of representations of wave packets in time 33

IV. Two coupled channels 42

A. Coupled-channel physics 42

B. The multi-channel Hamiltonian 43

C. Classical coupled oscillators 45

D. Siegert pseudostates in two coupled channels 48

E. Feshbach resonance 53

F. Analytical representation of the S-matrix in a coupled square well model 54

G. Feshbach resonances in a spectrum of Siegert pseudostates 60

H. Tuning Feshbach resonances 61

V. Conclusions 63

A. General discussion of the findings 63

B. Future directions 64

A. Finite element basis 64

B. Contrasting SPS theory with standard quantum mechanics 65

References 67

I. ACKNOWLEDGMENTS

The major creative insights discussed in this thesis were made by Robin Santra, Chris Greene, and a multitude of other physicists and mathematicians with emphasis weighted on those in the bibliography. The composition of an honors thesis was an opportunity to observe these thinkers solving problems. This composition should be viewed as the final draft of the notes of my observances and the presentation of the results of our numerical experiments.

The opportunity to work with Robin Santra and Chris Greene on this research has had an incredible influence on my development as a physicist. It has given me a deeper understanding of the physical world on the atomic scale, as well as many additions to the box of tools I will use to solve physical problems. I have gained insight into the challenges and successes of modern physics and have been inspired to continue with research. I thank Chris and Robin for their time, energy, and patience. Few students are lucky enough to meet such excellent teachers.

Financial support by the U.S. Department of Energy, Office of Science has made a significant contribution to this research.

II. INTRODUCTION

The understanding of scattering events is of central concern in the study of the physical world. The interaction of particles as they scatter from one another gives a valuable glimpse at the nature of the particles themselves. In our attempts to understand the underlying physics, it is essential that we are able to both create and explain the behavior of particles as they experience each other. In this study, we discuss a theoretical technique for explaining scattering events.

In some situations it may be sufficient to identify a particular shape or Feshbach resonance [1] [2] [3]. The concepts of shape and Feshbach resonance will be discussed in later sections. The calculation of resonances is commonly achieved by identifying the poles of the S, or scattering matrix [1] [2] [3]. Other purposes may necessitate the identification of an entire energy spectrum, and perhaps the associated wave functions, which requires the complete set of solutions to the time-independent Schrödinger equation (TISE), and will, in most

contexts, present a differential equation for which closed-form solutions simply do not exist. Further, a general Hamiltonian will give rise to a discretized spectrum of negative energy solutions, and a continuum of positive energy solutions. A realistic unbound physical state with uncertainty in both position and momentum will be a superpositon of these eigenstates of the Hamiltonian. A mathematical representation of such a physical state will require a summation over the discretized bound eigenstates weighted by expansion coefficients, and an integration over the continuous portion of the spectrum multiplied by a weighting function. In practical calculations, it is often necessary to perform the integration over the energy continuum numerically, which equates to approximating the integral as a discrete sum. For this reason, theorists have sought a method for discretizing the energy spectrum in a manner that preserves all the physics but is simpler to treat mathematically. Once a physical state has been represented as a superposition of eigenstates of the Hamiltonian, time evolution can be considered. This is often the most complete description of a scattering event, and the most challenging from a theoretical point of view.

The formalism of Siegert states (SSs) and Siegert pseudostates (SPSs) began in the 1930's with Siegert [4] in his studies of nuclear scattering events. The formalism has evolved to address the major issues of scattering theory discussed above—namely, the attainment of a discretized set of bound states as well as a discretized representation of the energy continuum forming a basis to the space of scattering events. The formalism also allows for accurate time evolution of a physical state. A Siegert state is defined [5] as a solution to the TISE,

$$\hat{H}\varphi(r) = E\varphi(r), \tag{1}$$

obeying vanishing at the origin

$$\varphi(0) = 0, \tag{2}$$

and the asymptotic boundary condition known as the Siegert boundary condition

$$\frac{d}{dr}\varphi(r)\bigg|_{r\to\infty} = ik\varphi(r \to \infty), \tag{3}$$

where k, the wave number, is complex [4] [6] [7] [8], in general, and is related to the energy by

$$E = \frac{k^2}{2}. \tag{4}$$

Note that one must divide $\varphi(r)/r$ to obtain the physical position representation of a SS; $\varphi(r)$ plays the role of $U(r)$ in the textbook derivation of the eigenstates of the hydrogen atom.

Also note that atomic units ($\hbar = 1$, $m_e = 1$) are used throughout this study, and consideration is limited to s-wave scattering, wherein the Hamiltonian in position representation takes the form

$$\hat{H} = -\frac{1}{2}\frac{d^2}{dr^2} + \hat{V}(r) \ . \tag{5}$$

It is beneficial to limit our discussion to cases of zero angular momentum because the relevant formal concepts can be conveyed. Generalizing to higher angular momentum states only affects the r-dependence of the problem in that it necessitates a modification of $V(r)$, resulting in an effective potential with a term accounting for centrifugal repulsion. Because the Siegert boundary condition only makes a demand on the r-dependence of the problem, the angular dependence can be treated with standard techniques, such as the partial wave expansion.

To understand the relevance of the Siegert boundary condition, we must consider the class of functions for which it is valid. First we note that it takes place at infinity, making the demand that at infinity the potential has stopped changing. Solutions to a radial Hamiltonian in the presence of a constant potential are spherical traveling wave fronts. These are represented by the function

$$\varphi(r \to \infty) \propto e^{ikr} \ , \tag{6}$$

which can be seen to obey the Siegert boundary condition (Eq. 3). We therefore know that Siegert states behave as spherical traveling wave fronts very far from the region of interaction.

One can calculate SSs by solving the TISE and demanding that solutions obey the boundary conditions of Eqs. (2) and (3). This technique is capable of capturing all types of interacting states: bound states, continuum states, and resonances. However, more recent theory often relies on computers to handle the numerics. The fact that the Siegert boundary condition takes place at infinity necessitates a modification of the treatment. One must find a smaller radius where the asymptotic boundary condition is applicable. At this final radius, r_f, we can make the demand that

$$\frac{d}{dr}\varphi(r)\bigg|_{r=r_f} = ik\varphi(r_f) \ . \tag{7}$$

The wave number here, like in the case of SSs, is complex. The energy is still related to the wave number by Eq. (4), so the application of this boundary condition results in a complex

energy spectrum. Siegert pseudostates (SPSs) are defined as solutions to the TISE obeying vanishing at the origin, as well as this form (Eq. 7) of the Siegert boundary condition. This study will focus of SPSs rather than SSs; from this point forward, cursive phi ($\varphi(r)$) will refer to the position representation of a Siegert pseudostate (SPS).

SPSs will be SSs in the presence of a radial potential that becomes constant by r_f. We refer to these potentials as cutoff potentials. If a cutoff potential becomes a constant other than zero, we can generalize Eq. (4) to read

$$E = \frac{k^2}{2} + V(r_f). \tag{8}$$

This modification essentially re-establishes the zero of our potential energy scale. If the potential is not constant by r_f, but is small, SPSs can be considered approximations to SSs, because the Siegert boundary condition will force the potential to a constant, damaging the continuity of the derivative.

For nuclear potentials, such as the Yukawa potential, this boundary condition is valid. Certain atomic scattering scenarios lend themselves to such a boundary condition. For collisions between atoms in their s-state, the long range behavior drops as $1/r^6$, which vanishes sufficiently fast to allow for application of the Siegert boundary condition at some r_f small enough to render numerical treatment tractable. However, ionic potentials are Coulombic far away, and the Coulomb potential vanishes slowly. The formalism of SPSs, as it currently stands, is not capable of providing accurate solutions to Coulomb problems. Also, the $1/r^2$ tail of the effective potential due to centrifugal repulsion for $l > 0$ approaches zero slowly. It is for this reason that we consider s-waves in this study. Still, the formalism is very powerful as a theoretical tool for handling the challenges of many scattering scenarios. Bound states and resonances are easily identified in spectra of Siegert pseudostates, and the continuum is necessarily discretized by the nature of the boundary condition. To refer to the discrete spectrum of closely-spaced positive-energy states, we introduce the term "pseudocontinuum". SPSs are shown to comprise a basis to the space of scattering states of one- and two-channel central potentials. Time evolution is easily implementable, as we shall see.

We proceed to develop the formalism of Siegert pseudostates. We will first rigorously derive Siegert pseudostates and analyze one-channel k and energy spectra. We will then treat orthogonality, completeness and time evolution in one channel before broadening our

consideration to a two-channel case. We will analyze the energy spectrum of a two-channel model to identify Feshbach resonances.

III. FORMAL CONCEPTS IN ONE-CHANNEL

Within this section, our goals are to elaborate on the techniques used to calculate Siegert pseudostates in the one-channel case, to identify the types of states in a SPS spectrum, to address the issue of completeness within the basis of SPSs, and to explore evolution in time.

A. Derivation of Siegert pseudostates

In solving the TISE subject to the Siegert boundary condition, we arrive at a generalized eigenvalue problem whose solutions are Siegert pseudostates. We must solve

$$\hat{H}\varphi(r) = E\varphi(r) \ , \tag{9}$$

with

$$\hat{H} = -\frac{1}{2}\frac{d^2}{dr^2} + \hat{V}(r) \ , \tag{10}$$

and solutions obeying

$$\varphi(0) = 0 \ ; \tag{11}$$

$$\frac{d}{dr}\varphi(r)\bigg|_{r=r_f} = ik\varphi(r_f). \tag{12}$$

With the aim of solving the problem numerically, we expand our solution into a representation in a primitive basis set, that is, a basis set that is convenient for numerical purposes. For the sake of generality, we allow for a set of non-orthogonal basis functions.

$$\varphi(r) = \sum_{j=1}^{N} c_j y_j(r). \tag{13}$$

The basis is assumed to be complete on the interval $[0, r_f]$ in the limit $N \to \infty$. A discussion of our choice of $y_j(r)$ is in Appendix A. In selecting a finite N, we effectively truncate the infinite dimensional vector space of solutions and consider an N-dimensional subspace.

To find matrix elements, we insert our ansatz into the TISE (Eq. 9), multiply from the left by an alternate element of our basis, and integrate over the region of consideration.

$$-\frac{1}{2}\int_0^{r_f} y_i(r)\frac{d^2}{dr^2}\sum_{j=1}^{N} c_j y_j(r)dr \quad + \int_0^{r_f} y_i(r)\hat{V}(r)\sum_{j=1}^{N} c_j y_j(r)dr$$
$$= E\int_0^{r_f} y_i(r)\sum_{j=1}^{N} c_j y_j(r)dr \ . \tag{14}$$

Next we relate energy to momentum (Eq. 8) and perform partial integration on the integrand containing the kinetic energy operator. We arrive at

$$\sum_{j=1}^{N} \left[-\frac{1}{2}y_i(r)\ \frac{d}{dr}y_j(r)\Big|_0^{r_f} + \frac{1}{2}\int_0^{r_f}\frac{d}{dr}y_i(r)\frac{d}{dr}y_j(r)dr + \int_0^{r_f} y_i(r)\hat{V}(r)y_j(r)dr\right] c_j$$
$$= \left(\frac{k^2}{2} + V(r_f)\right)\left[\sum_{j=1}^{N}\int_0^{r_f} y_i(r)y_j(r)dr\right] c_j \ . \tag{15}$$

As a result of partial integration, a derivative is evaluated at the surface. We use this opportunity to apply the Siegert boundary condition (Eq. (12)). It is this decision that eliminates the Hermiticity of our Hamiltonian, allowing for a complex eigenvalue. This is the only place in the derivation where the boundary condition enters. We can now define several $N \times N$ matrices by their elements:

$$\tilde{H}_{ij} = \int_0^{r_f}\frac{d}{dr}y_i(r)\frac{d}{dr}y_j(r)dr \tag{16}$$
$$+2\int_0^{r_f} y_i(r)\left[\hat{V}(r) - V(r_f)\right] y_j(r)dr \ ,$$
$$L_{ij} = y_i(r_f)y_j(r_f) \ , \tag{17}$$
$$Y_{ij} = \int_0^{r_f} y_i(r)y_j(r)dr \ . \tag{18}$$

$\tilde{H}$ is used to indicate that the matrix elements are not of the standard Hamiltonian, but are the elements after the kinetic energy operator has been modified by partial integration, and multiplied by a factor of two. With these definitions we can write our equation as a matrix equation, or more specifically, a non-linear eigenvalue problem of the dimension specified by our choice of N.

$$\left(\underline{\tilde{H}} - ik\underline{L} - k^2\underline{\mathrm{Y}}\right)\bar{c} = \bar{0} \ . \tag{19}$$

Underscores indicate matrices. $\bar{c}$ is the vector of coefficients from the expansion into the primitive basis set (Eq. (13)). Note that the matrices in this non-linear eigenvalue problem

are real and symmetric, while the eigenvalue is complex. This shows us that the eigenvectors must be complex. But, because the matrices are real, any eigenpair (k_n,$\bar{c}_n$) solving Eq. (19) also has a conjugate pair (k_n^*, $\bar{c}_n^*$) which solves the equation. These solutions can be found using iterative techniques, but iterative techniques are inefficient. A more elegant approach was introduced by Tolstikhin, Ostrovsky and Nakamura [5]. The goal is to arrive at a generalized eigenvalue problem of doubled dimension. Ref. [5] showed that this can be accomplished in the following way. We first define a vector

$$\bar{d} = ik\bar{c}. \tag{20}$$

We can then write Eq. (19) as

$$-\underline{\tilde{H}}\bar{c} = ik\left(\underline{Y}\bar{d} - \underline{L}\bar{c}\right). \tag{21}$$

We must capture this equation, and the definition of $\bar{d}$, in the generalized eigenvalue problem. To ensure the symmetry of the matrices, we choose to capture the definition of $\bar{d}$ as

$$\underline{Y}\bar{d} = ik\underline{Y}\bar{c}. \tag{22}$$

This leads to a symmetric generalized eigenvalue problem with real matrices but a complex eigenvalue, therefore giving rise to complex eigenvectors. We can capture all of the relevant information in

$$\begin{pmatrix} -\underline{\tilde{H}} & \underline{0} \\ \underline{0} & \underline{Y} \end{pmatrix} \begin{pmatrix} \bar{c} \\ \bar{d} \end{pmatrix} = ik \begin{pmatrix} -\underline{L} & \underline{Y} \\ \underline{Y} & \underline{0} \end{pmatrix} \begin{pmatrix} \bar{c} \\ \bar{d} \end{pmatrix}. \tag{23}$$

Notice that the first row of each matrix multiplied by the eigenvector gives rise to Eq. (21), and the second row multiplied by the eigenvector gives rise to the definition of $\bar{d}$, Eq. (20), in the form of Eq. (22). This generalized eigenvalue problem is easily handled by subroutines from standard linear algebra libraries [9] [10]. Its solutions ($\bar{c}$) are Siegert pseudostates. If they are left in the form of a vector, they are often referred to as Siegert pseudovectors. If multiplied by the position-space basis functions (Eq. (13)), they generally take on the name Siegert pseudostates. In practice, however, both representations receive both names. We noted that Eq. (19) had more than N solutions due to the real nature of the matrices and the complex nature of the eigenpairs of solutions. Upon diagonalization of Eq. (23), exactly $2N$ Siegert pseudostates are obtained. Are all $2N$ solutions necessary to comprise a basis? If not, how do we identify a complete set? Before addressing the issue of completeness, we will focus on the utility of the generalized eigenvalue problem of Eq. (23) in obtaining k-spectra, energy spectra, and resonances.

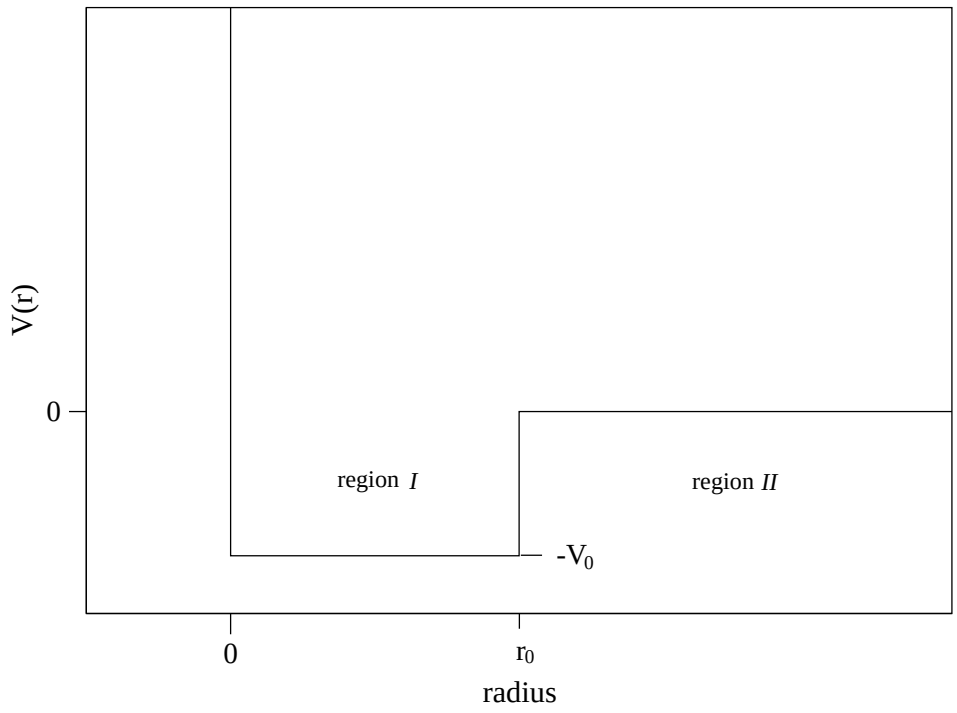

FIG. 1: The step potential of Eq. (24).

B. k spectrum and E spectrum of a central square well

We will now diagonalize Eq. (23) in the presence of a square-well potential in order to analyze the k and energy spectra, as well as view the position representation of a sample SPS. The step potential has the form

$$V(r) = -V_0\Theta(r_0 - r) \ , \tag{24}$$

where V_0 is a real, positive constant. The potential is shown in Fig. 1. We will revisit this model potential several times in this study. Using it to make the elements of the $\tilde{H}$-matrix, we construct Eq. (23). The resulting k and energy spectra are shown in Figs. 2, 3 and 4. The constituents of the spectra can be grouped into four categories. The states along the positive imaginary k axis are bound states. On the negative imaginary k axis are antibound or virtual states. Both bound and antibound states appear on the negative real energy axis. Bound and antibound states are graphically indistinguishable in the complex energy plane. For this reason it is often more useful to analyze the k plane. It is important to distinguish between bound and antibound states because they have quite different behavior.

If we consider a Siegert pseudostate at or beyond the boundary we see that

$$\varphi(r) \propto e^{ikr}. \tag{25}$$

where $r \geq r_f \geq r_0$. In the case of bound states, this can be written

$$\varphi(r) \propto e^{-|k|r} \ , \tag{26}$$

which displays the decaying exponential behavior of a negative-energy solution. However, in the case of an antibound state we find

$$\varphi(r) \propto e^{|k|r} \ , \tag{27}$$

which shows exponential growth. Because our solutions are only defined on the region $0 \leq r \leq r_f$, antibound states remain square integrable. However, they are often regarded as unphysical solutions. The remaining groups of states can be classified as either outgoing or incoming states. The outgoing states have $\mathrm{Re}(k) > 0$ corresponding to waves traveling radially away from the origin. These states comprise the branch of the spectrum with $\mathrm{Im}(E) < 0$ in the energy plane. The incoming states have $\mathrm{Re}(k) < 0$ corresponding to waves traveling toward the origin. Both incoming and outgoing waves are associated with complex k-values having the property $\mathrm{Im}(k) < 0$. Like the antibound states, this leads to exponential growth. Still, the solutions are square integrable on the interval $0 \leq r \leq r_f$. These four groups—bound, antibound, incoming, and outgoing—constitute the entire spectrum of SPSs.

It is beneficial to demystify the Siegert pseudostates themselves before we delve further into formal concepts. Fig. (5) shows an example of an outgoing Siegert pseudostate present in the square well. It is very sinusoidal in character, like the standard eigensolutions to the square well. Note, however, that it grows in amplitude as r increases. This is due to the negative imaginary part of the wave number.

C. Shape resonance

Before digression to another model potential, it is useful to engage in a brief discussion of the phenomenon of shape resonance. Resonances, in general, are positive-energy states with bound-state like properties. Potentials with barriers can temporarily trap interactions, forming quasibound states. Because the shape of the potential must include a barrier, and

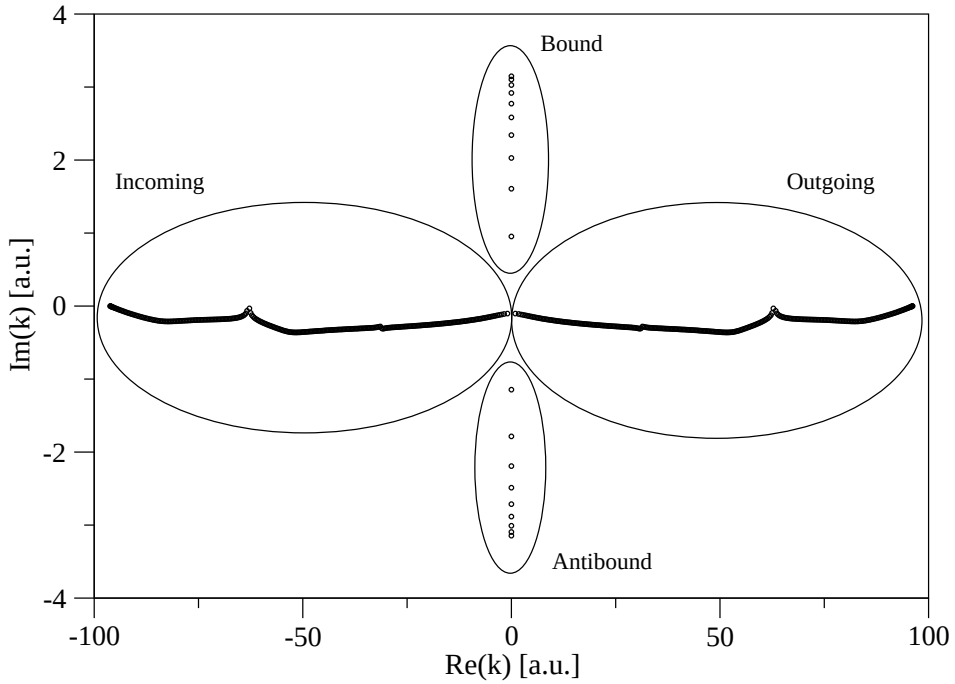

FIG. 2: The entire complex k spectrum for a particle in the step potential of Eq. (24) with $V_0 = 5$, $r_0 = 10$, and $N = 604$. The spectrum is entirely discrete. Ten bound states [$\mathrm{Re}(k) = 0$, $\mathrm{Im}(k) > 0$] are present, as well as ten antibound (nine of which are shown) [$\mathrm{Re}(k) = 0$, $\mathrm{Im}(k) < 0$]. The positive $\mathrm{Re}(k)$ branch of the spectrum shows the complex wave numbers of the outgoing Siegert pseudostates, the negative $\mathrm{Re}(k)$ branch the incoming. Notice the symmetry about the imaginary axis due to the fact that conjugate pairs of k-values satisfy Eq. (23).

because the shape of the barrier determines the energy of the quasibound state, resonances of this class are referred to as shape resonances.

Scattering theory can be carried out entirely in the context of real energies, but it is often very useful to map energies onto the complex energy plane. The imaginary part of a state's energy becomes informative. One can make use of a scattering cross section as a function of energy. In general, a scattering cross section measures the ratio of particles being absorbed in a scattering scenario to the number of particles entering a scattering scenario. From a scattering cross section, one can tell if the incident particles met with the target particles and interacted or if the incident particles passed right through. An example scattering cross section is shown in Fig. 6. The peaks mark resonances. These are places where incident particles are interacting with the target rather than simply passing through.

Though we may be dealing with complex energies, a particle always has only a real energy.

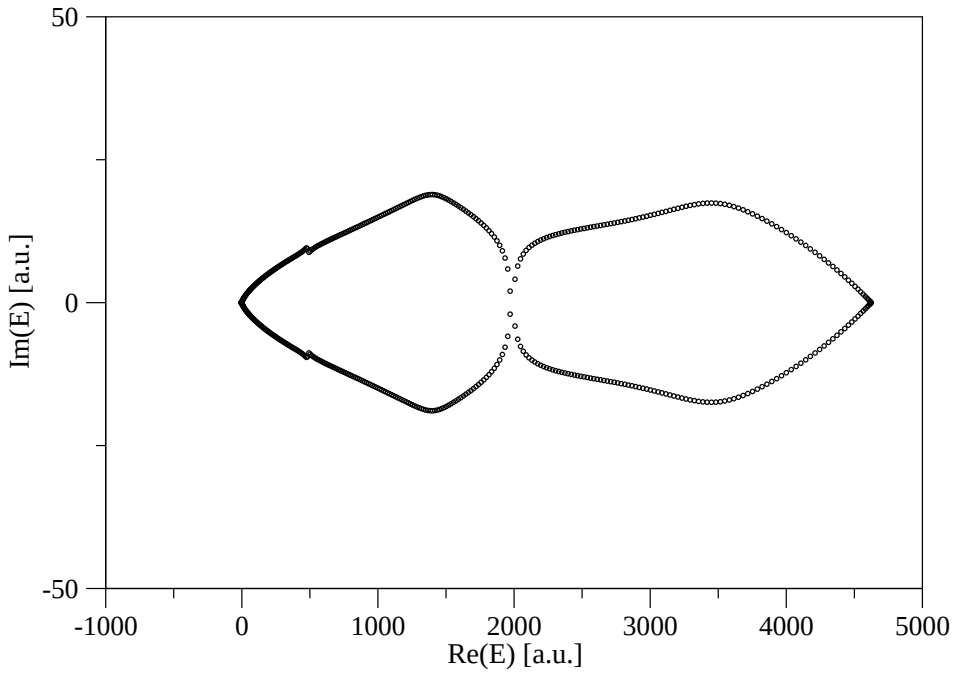

FIG. 3: The entire complex energy spectrum for a chosen number of basis functions, N, for a particle in the step potential of Eq. (24) with the same parameters as Fig. 2. Because the spectrum of SPSs is entirely discrete, increasing N increases the magnitude of energies considered. The portion close to the origin (Fig. 4) will be converged, while the higher energies may not.

In an experiment, one will generally vary the energy of the incident particles (corresponding to the real part of the energy mathematically) and observe the number of interactions taking place. In this way, one obtains a scattering cross section. When the energy of the incident particles is at the energy of a particular resonance, a peak will occur in the cross section. Notice the multitude of peaks in Fig. 6 corresponding to a large number of resonances. The real part of the energy corresponds to the energy of a resonance, but the imaginary part of the energy corresponds to the width of the peak in the cross section. An idealized peak in a scattering cross section is shown in Fig. 7. Narrow peaks correspond to well-defined resonance energies. One can see from the uncertainty relation between energy and time,

$$\Delta E \Delta t \geq \frac{\hbar}{2} \,, \tag{28}$$

that the more sharply defined a state's energy is (the smaller ΔE is), the less sharply defined its lifetime must be (the larger Δt must be). Because the uncertainty in time grows, the mean lifetime of a resonant state grows. Resonances are identified as sharp peaks in a scattering cross section corresponding to well-defined energies and long lifetimes.

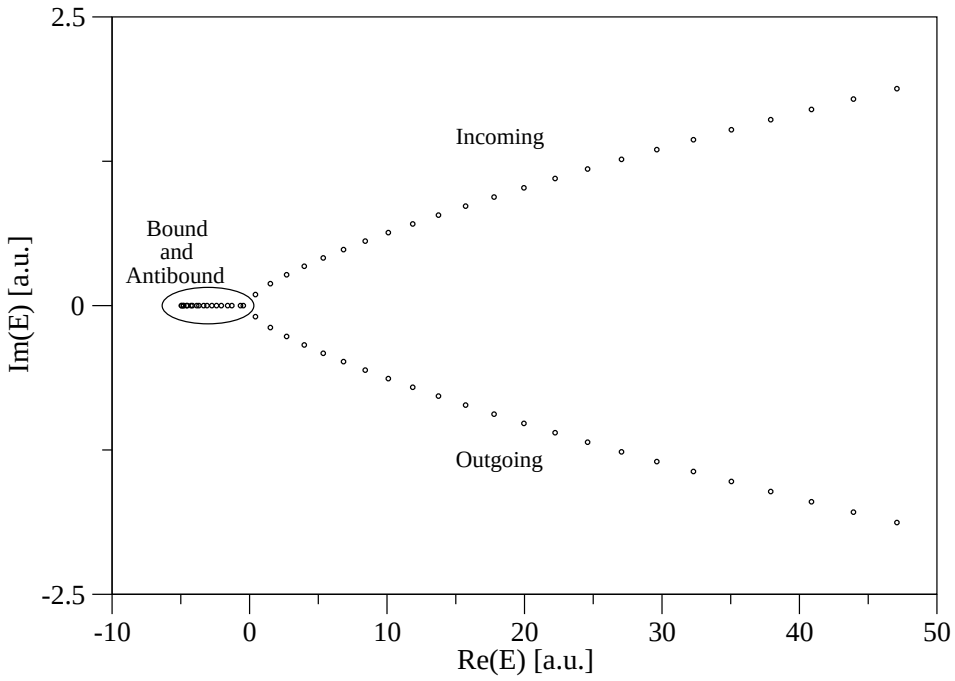

FIG. 4: The converged portion of the complex energy spectrum for a particle in the step potential of Eq. (24) with the same parameters as Fig 2. The bound and antibound states are on the negative real energy axis. The branches of outgoing and incoming Siegert pseudostates are labeled. This figure shows a small portion of the total energy spectrum. The total energy spectrum is shown in Fig. 3. It should be noted that, because this energy spectrum is in the presence of a cutoff potential, and because we have chosen r_f to lie in the region of constant potential, these SPS energies are also SS energies.

Another way to explain the characteristic long lifetime of resonant states is to look at their evolution in time. We can write the complex energy as

$$E = E_{Re} - i\frac{\Gamma}{2} \, , \tag{29}$$

where Γ corresponds to the width of the resonance in the scattering cross section (see Fig. 7). A state evolving in time in the standard exponential way can be written as

$$\psi(r,t) = \psi(r)e^{-iEt} = \psi(r)e^{-iE_{Re}t}e^{-\frac{\Gamma}{2}t} \, . \tag{30}$$

We see that while this state has decaying behavior in time, because the imaginary part of the energy of the resonance is so small, the lifetime will be orders of magnitude longer than the characteristic time scale of other scattering events, such as particles with energy off

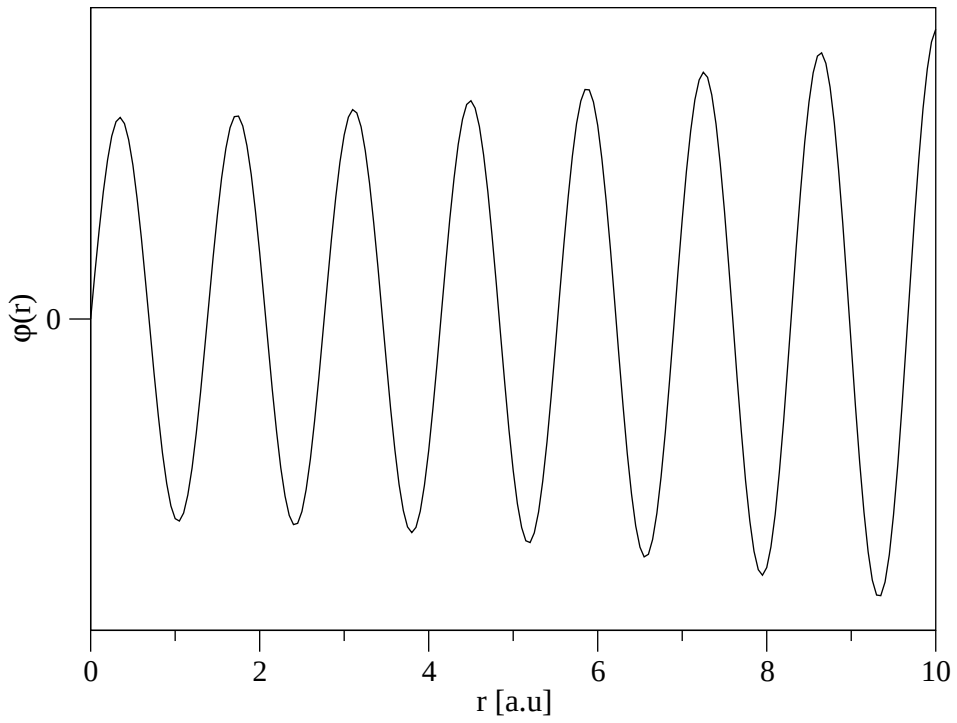

FIG. 5: An example of the real part of a Siegert pseudostate. The SPS shown is outgoing and has energy $E \approx 5.4 - .41i, k \approx 3.3 - .13i$ in atomic units. Note the growth as r increases, caused by $\mathrm{Im}k < 0$.

resonance that simply pass by the target. It is for this reason that resonances are referred to as quasibound states.

D. Shape resonance in the Bain potential

Now we seek a resonance in a model potential. Here we consider the spectrum of energies of Siegert pseudostates present in the Bain potential, where

$$V(r) = V_0 r^2 e^{-\frac{r}{\gamma}} \ . \tag{31}$$

In Fig. 8 we see the barrier present in the Bain potential which gives rise to shape resonances. This model potential is of particular interest in this portion of our study for several reasons. The first, and qualifying reason, is that it is an effective cutoff potential. By effective cutoff potential, we refer to the fact that the decaying exponential behavior drops the potential effectively to zero within a radius that allows for practical numerical treatment. The potential also has a maximum at a finite radius on the interval $[0, r_f]$. This structure

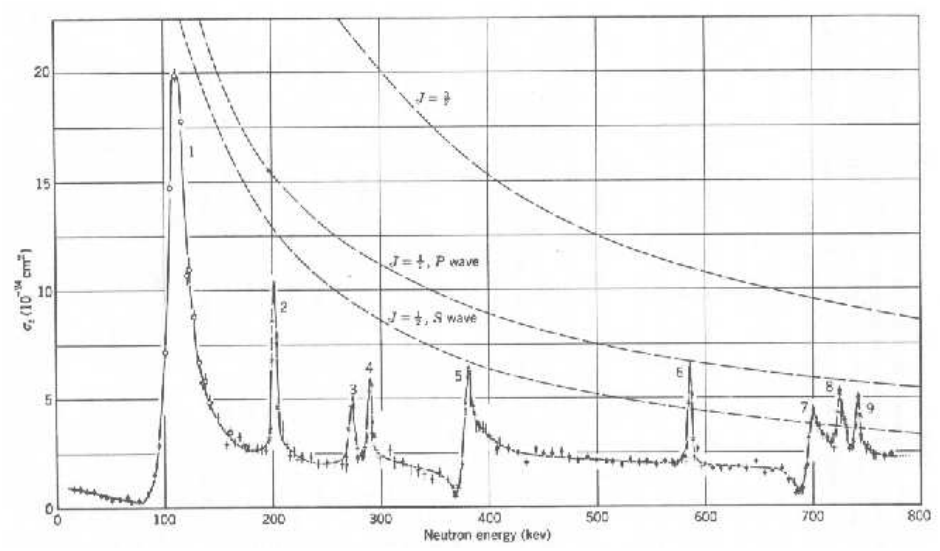

FIG. 6: An example scattering cross section. This example considers incident neutrons interacting with sulfur. Peaks in the scattering cross section correspond to energies of neutrons that have a high probability of being scattered by sulfur. This image was obtained from Ref. [11].

will give rise to shape resonances, providing a case for testing the formalism. In particular, one of the shape resonances has been explored in detail in Ref. [5], wherein an orthonormal primitive basis set provided the numerical foundation. We now compare the results from our numerical tests with the established results of Ref. [5].

In Eq. (31) we choose the parameters $V_0 = 15/2, \gamma = 1$, giving the potential a maximum at $r = 2$, where $V(2) \approx 4.06$. We choose $N = 604$ and $r_f = 25$. Upon diagonalization, we obtain the energy spectrum shown in Fig. 9. The Bain potential has the quality $V(r) \geq 0$, so bound and antibound states are not present. However, by analogy to the spectrum of the step potential, one can identify the branches of the energy spectrum corresponding to incoming and outgoing Siegert pseudostates. We see the shape resonance of interest lying separate from the pseudocontinuum of energy eigenvalues. The complex energy of the resonance has a much smaller imaginary part, characterizing it as a resonance. Upon investigation of the exact location of the energy of the resonance in the complex energy plane, we find it lies at $E = 3.42639031 - .012774480i$. Here, it is identified to the number of decimal places with which it agrees with the value calculated in Ref. [5]. We see that our accuracy is more than enough for practical calculations. The energy of the resonance is shown relative to the potential in Fig. 8.

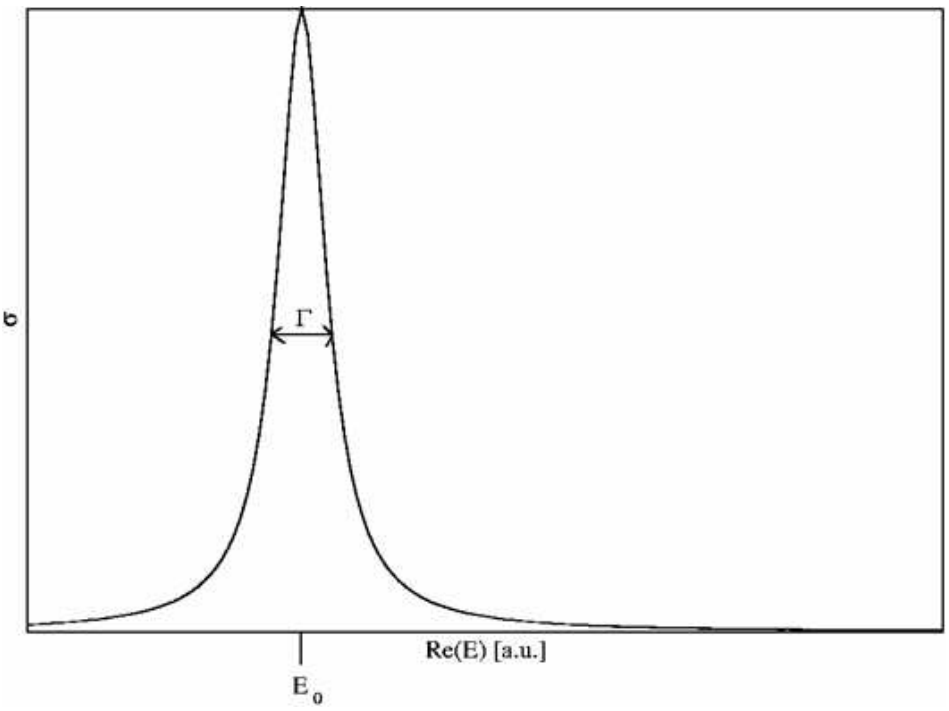

FIG. 7: An idealized scattering cross section depicting one resonance. The width of the resonance is determined by the imaginary part of the particle's complex energy. The narrower the resonance, the longer the lifetime.

E. Orthogonality and completeness

Now, more familiar with elements of relevant nomenclature and comfortable with example spectra, we move our study forward to consider other aspects of the formalism, namely orthogonality, completeness and time evolution. First we derive the orthogonality condition obeyed by Siegert pseudostates. The outline of the derivation is as follows: we transform the generalized eigenvalue problem of Eq. (23)—where the matrices are real and symmetric—into a standard eigenvalue problem with a complex symmetric matrix, keeping track of the way the modifications to the matrices modify the eigenvectors. Then, with many properties of eigenvectors of a complex symmetric eigenvalue problem understood, we can work backward to gain insight into the properties of the eigenvectors of the generalized eigenvalue problem.

We begin with Eq. (23) which can be written

$$\underline{A}\bar{x} = ik\underline{B}\bar{x} \tag{32}$$

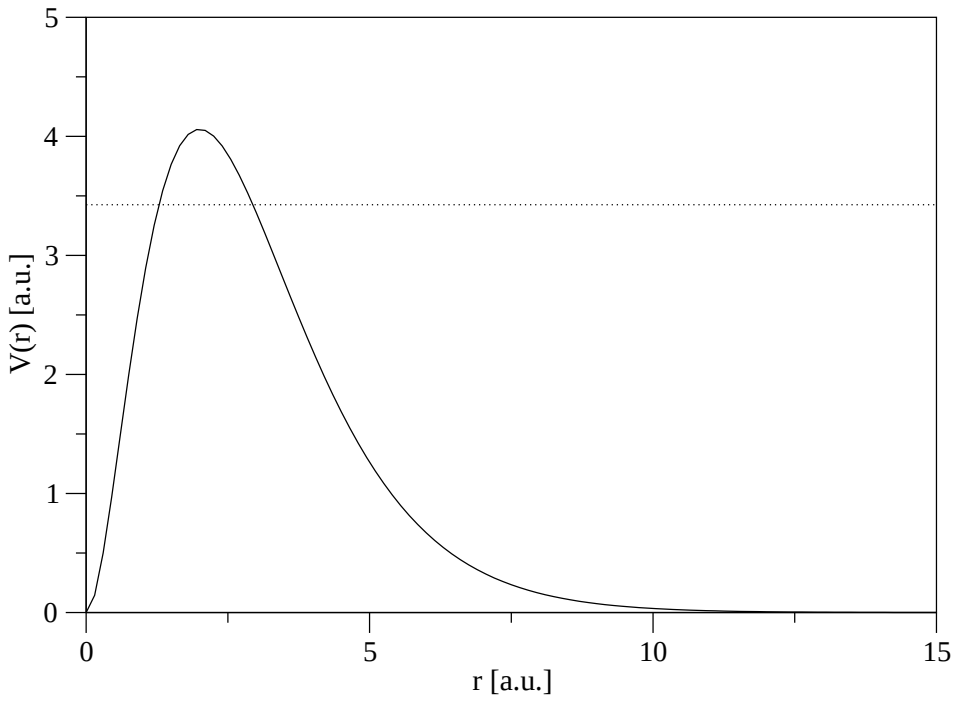

FIG. 8: The Bain potential. The energy of the resonance is marked with a dotted line. The potential peaks at $r = 2$ and vanishes by a finite r_f. A particle may resonate in the region behind the barrier.

where

$$\underline{A} = \begin{pmatrix} -\underline{\tilde{H}} & \underline{0} \\ \underline{0} & \underline{Y} \end{pmatrix} , \tag{33}$$

$$\underline{B} = \begin{pmatrix} -\underline{L} & \underline{Y} \\ \underline{Y} & \underline{0} \end{pmatrix} , \tag{34}$$

and $\bar{x}$ is the column vector containing the coefficients of expansion into the primitive basis set. Explicitly,

$$\bar{x} = \begin{pmatrix} \bar{c} \\ \bar{d} \end{pmatrix} . \tag{35}$$

Because the generalized eigenvalue problem has dimension $2N \times 2N$, $\bar{x}_i$ is a vector of length $2N$, and i runs from 1 to $2N$. In other words, there are $2N$ vectors satisfying Eq. (23). There are also $2N$ k-values, making $2N$ total eigenpairs of solutions to Eq. (23). We can define the matrices

$$\underline{X} = [\bar{x}_1, \ldots, \bar{x}_{2N}] \in \mathbb{C}^{2N \times 2N} , \tag{36}$$

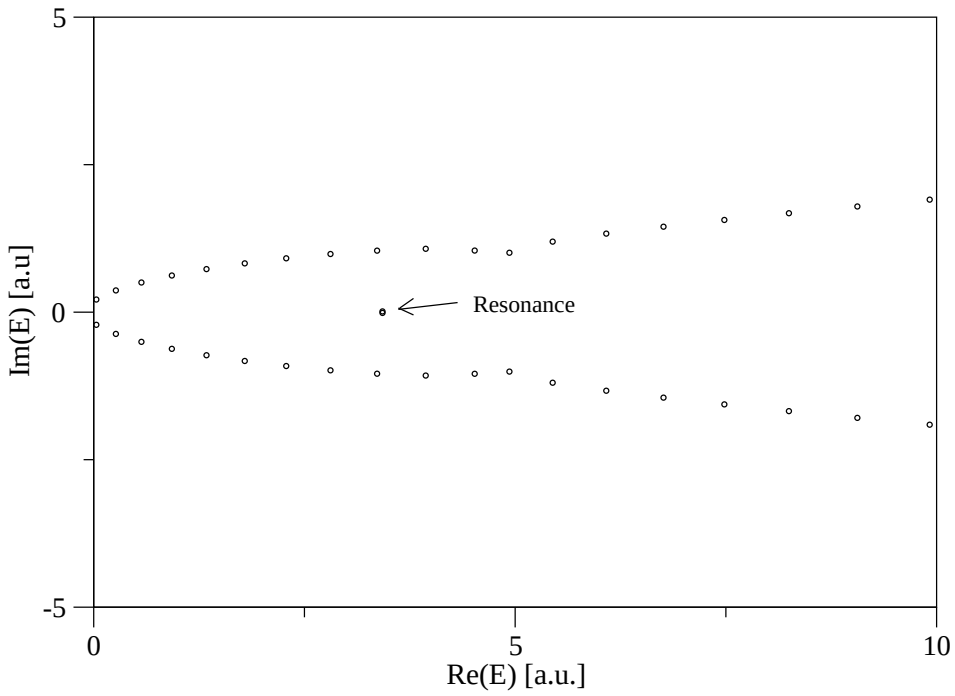

FIG. 9: The energy spectrum of the Bain potential (Eq. (31), Fig. (8)). Notice the resonance energy with small imaginary part lying separate from the pseudocontinuum. The point labeled as the resonance is actually two circles nearly on top of each other—one corresponding to an outgoing, one to an incoming SPS.

and

$$\underline{K} = \mathrm{diag}\,[ik_1, \ldots, ik_{2N}] \in \mathbb{C}^{2N\times 2N} \; . \tag{37}$$

We can now write

$$\underline{AX} = \underline{BXK} \; . \tag{38}$$

The overlap matrix $\underline{Y}$ is real and symmetric. In addition, all of its eigenvalues are positive. These statements taken together inform us that $\underline{Y}$ is positive definite. A consequence of the positive definiteness of $\underline{Y}$ is that $\underline{Y}^{-1}$ exists. This is all the information we need to construct $\underline{B}^{-1}$. After explicit construction,

$$\underline{B}^{-1} = \begin{pmatrix} \underline{0} & \underline{Y}^{-1} \\ \underline{Y}^{-1} & \underline{Y}^{-1}\underline{L}\underline{Y}^{-1} \end{pmatrix} \; . \tag{39}$$

It is important to note that $\underline{B}$ is invertible because it demands that all matrices similar to $\underline{B}$ are also invertible. The invertibility of $\underline{B}$ is a cornerstone of this derivation. Because we make direct use of the invertiblity of the matrix $\underline{B}$ at the outset of this derivation, we

expect to arrive at an orthogonality condition and a completeness relation in terms of $\underline{B}$ or its inverse.

Because $\underline{B}$ is a real, symmetric matrix (a type of Hermitian matrix), it can be diagonalized under a similarity transformation of the form

$$\underline{U}^T \underline{B} \underline{U} = \underline{D} \,, \tag{40}$$

where $\underline{U} \in \mathbb{R}^{2N \times 2N}$ has the property

$$\underline{U}^T \underline{U} = \underline{\mathbb{1}} \,, \tag{41}$$

and $\underline{D}$ is a diagonal matrix containing real, non-zero positive and negative elements along its diagonal. This is known because $\underline{D}$ is similar to $\underline{B}$ and therefore, as mentioned above, must be invertible. Because $\underline{D}$ is real and invertible, we can utilize the matrices $\underline{D}^{1/2}$, $\underline{D}^{-1/2}$, and $\underline{D}^{-1}$ in our derivation. Here the $1/2$ superscript indicates taking the square root of each element of $\underline{D}$, and the $-1/2$ superscript indicates taking the square root of each element of $\underline{D}^{-1}$. Notice that $\underline{D}^{1/2}$ and $\underline{D}^{-1/2}$ are both diagonal matrices with some elements real, some imaginary. This will be the source of complexity in our final eigenvalue problem.

We now proceed to transform Eq. (38) into a complex symmetric eigenvalue problem. We insert $\underline{B} = \underline{U D U}^T$ into Eq. (38) and operate from the left with $\underline{D}^{-1/2} \underline{U}^T$ to obtain

$$\underline{D}^{-1/2} \underline{U}^T \underline{A} \underline{X} = \underline{D}^{1/2} \underline{U}^T \underline{X} \underline{K} \,. \tag{42}$$

We now insert the identity matrix in the form of $\underline{U D}^{-1/2} \underline{D D}^{-1/2} \underline{U}^T$ between $\underline{A}$ and $\underline{X}$ and write $\underline{D}^{1/2}$ as $\underline{D D}^{-1/2}$. If we assign

$$\underline{\tilde{U}} = \underline{U D}^{-1/2} \,, \tag{43}$$

giving

$$\underline{\tilde{U}}^T = \underline{D}^{-1/2} \underline{U}^T \,, \tag{44}$$

then our equation reads

$$\underline{\tilde{U}}^T \underline{A \tilde{U} D \tilde{U}}^T \underline{X} = \underline{D \tilde{U}}^T \underline{X K} \,, \tag{45}$$

or

$$\underline{\tilde{A} \tilde{X}} = \underline{\tilde{X} K} \,, \tag{46}$$

with

$$\underline{\tilde{A}} = \underline{\tilde{U}}^T \underline{A \tilde{U}} \,, \tag{47}$$

and

$$\underline{\tilde{X}} = \underline{D\tilde{U}^T}\,\underline{X}\,. \tag{48}$$

We have now arrived at a standard eigenvalue problem (Eq. (46)) with the same eigenvalue matrix $\underline{K}$ but modified eigenvector matrix $\underline{\tilde{X}}$. Our goal is to study the properties of $\underline{\tilde{X}}$ in order to derive properties of $\underline{X}$.

Note that $\underline{\tilde{A}}$ is complex symmetric. It is not possible, in general, to guarantee that $\underline{\tilde{A}}$ is diagonalizable (see Ref. [12]). It will, however, be diagonalizable if all $2N$ eigenvalues are distinct. This demands that no two diagonal elements of the diagonal matrix $\underline{K}$ are the same. From our numerical experience with several potentials, we know this to be the case. We can therefore proceed with the sensible assumption that $\underline{\tilde{A}}$ is diagonalizable.

It is shown in Ref. [12] that for a standard eigenvalue problem wherein the matrix is complex symmetric and diagonalizable, the matrix of eigenvectors may be chosen to be complex orthogonal.

$$\underline{\tilde{X}}^T\,\underline{\tilde{X}} = \underline{\mathbb{1}}\,. \tag{49}$$

This statement of orthogonality indicates that the vectors comprising the matrix $\underline{\tilde{X}}$ are linearly independent, and therefore comprise a basis for $\mathbb{C}^{2N}$. We can therefore expand an arbitrary vector $\bar{\nu}$ in this basis.

$$\bar{\nu} = \sum_{n=1}^{2N} \alpha_n \bar{\tilde{x}}_n\,. \tag{50}$$

Making use of the orthogonality, we find

$$\alpha_m = \bar{\tilde{x}}_m^T \bar{\nu}\,. \tag{51}$$

Using this in Eq. (50), we find

$$\bar{\nu} = \sum_{n=1}^{2N} \bar{\tilde{x}}_n^T \bar{\nu} \bar{\tilde{x}}_n = \sum_{n=1}^{2N} \bar{\tilde{x}}_n \bar{\tilde{x}}_n^T \bar{\nu}\,, \tag{52}$$

from which we conclude

$$\sum_{m=1}^{2N} \bar{\tilde{x}}_m \bar{\tilde{x}}_m^T = \underline{\mathbb{1}}\,. \tag{53}$$

This is the completeness relation obeyed by the eigenvectors of the complex symmetric eigenvalue problem.

We can now use Eqs. (53) and (49) to derive relations between the eigenvectors of the generalized eigenvalue problem of Eq. (38). The completeness relation obeyed by the

eigenvectors of the generalized eigenvalue problem of Eq. (38) can be derived from Eq. (53). We use $\bar{\tilde{x}}_m = \underline{D\tilde{U}}^T \bar{x}_m$ and multiply from the left by $\underline{UD}^{1/2}$ and from the right by $\underline{D}^{-1/2}\underline{U}^T$ to arrive at

$$\underline{B} \sum_{m=1}^{2N} \bar{x}_m \bar{x}_m^T = \underline{\mathbb{1}} \ . \tag{54}$$

But because $\underline{B}^{-1}$ exists, we can write the completeness relation obeyed by the full vectors of the generalized eigenvalue problem of Eq. (38) as

$$\sum_{m=1}^{2N} \bar{x}_m \bar{x}_m^T = \underline{B}^{-1} \ . \tag{55}$$

We see the inverse of the matrix $\underline{B}$ enter into this completeness relation in a critical way.

To derive an expression for the orthonormality condition obeyed by Siegert pseudostates, we use the definitions of $\underline{\tilde{X}}$ and $\underline{\tilde{U}}$ in Eq. (49) to obtain

$$\underline{X}^T \underline{BX} = \underline{\mathbb{1}} \ , \tag{56}$$

which is equivalent to the expression

$$\bar{x}_m^T \underline{B} \bar{x}_n = 2ik_n \delta_{mn}, m, n = 1, \ldots, 2N \ . \tag{57}$$

The $2ik_n$ appearing in front of the Kronecker delta amounts to a rescaling of each vector by $1/\sqrt{2ik_n}$ and is the normalization convention of [5]. The ik essentially accommodates the ik from $\bar{d}$, and the factor of two allows for $k_m + k_n$ in the denominator. Carrying the multiplication of Eq. (57) through, we find

$$\bar{c}_m^T \underline{Y} \bar{c}_n + i \frac{\bar{c}_m^T \underline{L} \bar{c}_n}{k_m + k_n} = \delta_{mn} \ . \tag{58}$$

This is the orthonormality condition obeyed by Siegert pseudostates. We can return to the familiar position representation by using the definition of the overlap and surface matrices and recalling that

$$\sum_{i=1}^{N} c_{in} y_i(r) = \varphi_n(r) \ , \tag{59}$$

where n ranges from 1 to $2N$. Eq. (59) simply says that the product of the nth vector of coefficients (referred to as a Siegert pseudovector) with the vector of position-dependent basis functions gives the position representation of the nth Siegert pseudostate. Note that each of the $2N$ Siegert pseudovectors contains only N elements. The second N elements

constitute the vector $\bar{d}$, which gives us no new information because it is simply a complex multiple of $\bar{c}$. Using Eq. (59) we find

$$\int_0^{r_f} \varphi_m(r)\varphi_n(r)dr + i\frac{\varphi_m(r_f)\varphi_n(r_f)}{k_m + k_n} = \delta_{mn} \ . \tag{60}$$

The overlap matrix $\underline{Y}$ has effectively integrated the pseudostates over the interaction volume, and the surface matrix $\underline{L}$ has introduced a surface term.

Note the existence of a singularity when $k_m = -k_n$. This can only occur when the magnitude of a k-value of an antibound state is the same as the magnitude of a k-value of a bound state, because outgoing and incoming states are complex conjugates of each other. While there is nothing forbidding this occurrence, it is unlikely that the two will have matching magnitudes to machine precision. Also, note that in Eq. (60) complex conjugation does not occur in the overlap integral between the two states, even though the functions describing the states in position space are complex. The integral is only over the interaction region, rather than all space. This must be the case, because our solutions are only defined on this interval. A surface term also arises. The orthonormality condition of Eqs. (58) and (60) is a consequence of the boundary condition obeyed by SPSs. It differs from the orthonormality condition of standard quantum mechanics in the ways just mentioned. A more general discussion of the contrast between the formalism of Siegert pseudostates and the formalism of standard quantum mechanics will be held in Sec. B.

Before we can use our completeness relations to represent an arbitrary wave packet as a superposition of SPSs, it is useful to manipulate them a little more. Making explicit mention of the normalization factors, we write Eq. (55) as

$$\sum_{m=1}^{2N} \frac{1}{2ik_m} \begin{pmatrix} \bar{c}_m \\ \bar{d}_m \end{pmatrix} \left(\bar{c}_m^T \bar{d}_m^T\right) = \begin{pmatrix} \underline{0} & \underline{Y}^{-1} \\ \underline{Y}^{-1} & \underline{Y}^{-1}\underline{L}\underline{Y}^{-1} \end{pmatrix} \ . \tag{61}$$

Carrying the multiplication through offers three unique equations. We will make use of one of them:

$$\sum_{m=1}^{2N} \bar{c}_m \bar{c}_m^T = 2\underline{Y}^{-1} \ . \tag{62}$$

It is also beneficial to define

$$M_{mn} = \bar{c}_m^T \underline{Y} \bar{c}_n = \delta_{mn} - i\frac{\bar{c}_m^T \underline{L} \bar{c}_n}{k_m + k_n} = \int_0^{r_f} \varphi_m(r)\varphi_n(r)dr \ . \tag{63}$$

Now we have the tools we need to approach this derivation from the point of view of linear algebra as well as the point of view of calculus. In certain contexts, relations involving the

position representation of SPSs are more useful, whereas in other contexts it is more helpful to have expressions in terms of Siegert pseudovectors. In contexts where one representation is more appropriate than the other, the appropriate representation will be used. However, it is perhaps pedagogically valuable to demonstrate the expansion of a wave packet in both representations. For this portion of the study, the analogous steps will occur simultaneously.

We want to expand a vector (function) in the SPS basis. The vector $\bar{c}_n$ has N elements, and thus the vector we will expand will be of length N. A basis of $2N$ SPSs is overcomplete in $\mathbb{C}^N$, so we utilize N SPSs.

$$\bar{\nu} = \sum_{n=1}^{N} \alpha_n \bar{c}_n \ ; \tag{64}$$

$$\psi(r) = \sum_{n=1}^{N} \alpha_n \varphi_n(r) \ . \tag{65}$$

We seek the coefficients of expansion, α_n.

$$\bar{c}_m^T \underline{Y} \bar{\nu} = \sum_{n=1}^{N} \alpha_n \bar{c}_m^T \underline{Y} \bar{c}_n \ ; \tag{66}$$

$$\int_0^{r_f} \varphi_m(r)\psi(r)dr = \sum_{n=1}^{N} \alpha_n \int_0^{r_f} \varphi_m(r)\varphi_n(r)dr \ . \tag{67}$$

Notice the appearance of the $\underline{M}$-matrix.

$$\bar{c}_m^T \underline{Y} \bar{\nu} = \sum_{n=1}^{N} M_{mn} \alpha_n \ ; \tag{68}$$

$$\int_0^{r_f} \varphi_m(r)\psi(r)dr = \sum_{n=1}^{N} M_{mn} \alpha_n \ . \tag{69}$$

We utilize the notation

$$\underline{C} = [\bar{c}_1, \ldots, \bar{c}_N] \ , \tag{70}$$

and

$$\bar{\varphi}(r) = \begin{pmatrix} \varphi_1(r) \\ \vdots \\ \varphi_N(r) \end{pmatrix} \ . \tag{71}$$

The integral in Eq. (69) becomes N integrals, one for each $\varphi_i(r)$. Also, $\bar{\alpha}$ refers to the vector containing the coefficients of expansion into the SPS basis. Our equations read

$$\underline{C}^T \underline{Y} \bar{\nu} = \underline{M} \bar{\alpha} \ , \tag{72}$$

and

$$\int_0^{r_f} \bar{\varphi}(r)\psi(r)dr = \underline{M}\bar{\alpha} \ . \tag{73}$$

It is apparent at this point that we will have a unique expansion, that is, a unique $\bar{\alpha}$ for which Eqs. (72) and (73) hold if and only if the matrix $\underline{M}$ is invertible. If $\underline{M}$ is invertible, the selected subset of N SPSs utilized in the construction of the $\underline{M}$ constitute a basis for the vector space.

Once Eq. (23) has been diagonalized, construction of the matrix $\underline{M}$ is possible. The eigenvalues of $\underline{M}$ can then be found. Whether or not $\underline{M}$ is invertible is directly linked to its eigenvalue spectrum. If zero is one of the eigenvalues, the matrix is not invertible. We numerically seek eigenvalues in the case of an $N \times N$ $\underline{M}$-matrix, as well as in the case of a $2N \times 2N$ $\underline{M}$-matrix. In the case of an $N \times N$ matrix, all possible combinations of the branches of SPSs giving a total of N states have been considered. In the case where $\underline{M}$ is $N \times N$, zero is never in the spectrum. The existence of N eigenvalues equal to zero to machine precision when $\underline{M}$ contains contributions from all $2N$ SPSs confirms that $2N$ SPSs supply an overcomplete basis. The fact that $\underline{M}$ is invertible whenever it is an $N \times N$ matrix composed of contributions from complete branches of the SPS spectrum (as opposed to choosing an arbitrary combination of bound, antibound, outgoing and incoming SPSs totaling N states) confirms that any combination of the branches of SPSs totaling N states forms a complete basis for the space. Thus, there are at least four bases for the space:

$$\begin{matrix} \text{bound} + \text{outgoing} \\ \text{bound} + \text{incoming} \\ \text{antibound} + \text{outgoing} \\ \text{antibound} + \text{incoming} \end{matrix} \ .$$

Other combinations of SPSs totaling N may comprise a basis, but only these four sensible combinations have been tested.

We can now express $\bar{\alpha}$ as

$$\bar{\alpha} = \underline{M}^{-1}\underline{C}^T\underline{Y}\bar{\nu} \ ; \tag{74}$$

$$\bar{\alpha} = \underline{M}^{-1}\int_0^{r_f} \bar{\varphi}(r)\psi(r)dr \ ; \tag{75}$$

or

$$\alpha_m = \sum_{n=1}^{N} \left(\underline{M}^{-1}\right)_{mn} \bar{c}_n^T\underline{Y}\bar{\nu} \ , \tag{76}$$

$$\alpha_m = \sum_{n=1}^{N} \left(\underline{M}^{-1}\right)_{mn} \int_0^{r_f} \varphi_n(r)\psi(r)dr \ . \tag{77}$$

Allowed combinations of SPSs totaling N have been discussed, and the validity of $\underline{M}^{-1}$ has been established. We can write our expansions.

$$\bar{\nu} = \sum_{m=1}^{N}\sum_{n=1}^{N} \left[\left(\underline{M}^{-1}\right)_{mn} \bar{c}_n^T \underline{Y} \bar{\nu}\right] \bar{c}_m \ ; \tag{78}$$

$$\psi(r) = \sum_{m=1}^{N}\sum_{n=1}^{N} \left[\left(\underline{M}^{-1}\right)_{mn} (\varphi_n|\psi) \right] \varphi_m(r) \ . \tag{79}$$

In the last equality the round brackets represent an inner product without complex conjugation performed on the bra. Before we move forward to analyze the accuracy of Eqs. (78) and (79), we take a moment to identify the associated formal statement of completeness within the basis of N Siegert pseudovectors. We begin with Eq. (78), which we can write as

$$\bar{\nu} = \sum_{m=1}^{N}\sum_{n=1}^{N} \bar{c}_m \left(\underline{M}^{-1}\right)_{mn} \bar{c}_n^T \underline{Y} \bar{\nu} \ , \tag{80}$$

from which we conclude

$$\sum_{m=1}^{N}\sum_{n=1}^{N} \bar{c}_m \left(\underline{M}^{-1}\right)_{mn} \bar{c}_n^T = \underline{Y}^{-1} \ . \tag{81}$$

This is the minimal completeness relation within the basis of Siegert pseudosates. The summations include N contributions; four allowed groups of N SPSs have been discussed. This completeness relation allows us to quickly represent a vector in the SPS basis. We will demonstrate how to use Eq. (81) in the next subsection.

We have now expressed an arbitrary vector (function) in terms of Siegert pseudostates. In the process, we have reached the conclusion that N of the $2N$ SPSs, if chosen correctly, comprise a basis for the space. This was anticipated due to the nature of our derivation. We originally introduced an N-dimensional space, but quickly found ourselves with $2N$ basis vectors. Therefore, we expected a subset of the $2N$ solutions to the generalized eigenvalue problem (Eq. (23)) to span the space. Formally, we have shown this to be the case. We would like to confirm the completeness of selected subsets of N Siegert pseudostates with numerical tests.

F. Numerical validation of completeness

We have previously diagonalized the generalized eigenvalue problem of Eq. (23) in the presence of a radial step potential. We now place a wave packet in the potential and test the accuracy of its representation in the basis of Siegert pseudostates. The derivations in this section lend themselves to position representation.

We choose a Gaussian wave packet centered at radius ρ with characteristic width μ and momentum k_0 radially away from the origin.

$$\psi(r) = e^{\frac{-(r-\rho)^2}{2\mu^2} + ik_0(r-\rho)} \,, \tag{82}$$

which we can express as Eq. (79). Recall that the position representation of the SPSs is in terms of a set of primitive basis functions. To understand where the accuracy of our expansion fails, we must first evaluate the accuracy of our underlying primitive basis. In choosing a value of N, we choose the number of basis functions to be present in the interaction volume and also the dimension of the matrices defined by Eqs. (16)-(18). The choice of N therefore dictates how many SPSs are calculated upon diagonalization of Eq. (23), as well as the dimension of the matrix $\underline{M}$ (Eq. (63)). Our strategy for testing the completeness of the SPS basis is as follows. We first expand the wave packet in the primitive basis, choosing expansion coefficients to minimize a χ^2—call it χ_1^2. We then attempt to reproduce these expansion coefficients within the basis of Siegert pseudovectors. We calculate a second χ^2, χ_2^2, which evaluates the difference of the two representations of the expansion coefficients. Finally, we reconstruct the wave packet with the coefficients of expansion into the SPS basis and calculate χ_3^2 to compare the reconstruction to the initial wave packet. We anticipate that as we increase N for a given r_f, we should see χ_1^2 converge to a value very close to zero. χ_2^2, however, ought to be close to zero regardless of the choice of N, because our claim is that the SPSs span the vector space whose dimension is set by the choice of N. If χ_2^2 behaves as we predict, we should see χ_3^2 match χ_1^2 for all values of N. While χ_2^2 and χ_3^2 will test the accuracy of an expansion in terms of N vectors, we would also like to test the accuracy of an expansion in terms of all $2N$ Siegert pseudovectors. χ_4^2 and χ_5^2 provide analogous information to χ_2^2 and χ_3^2, except with respect to expansion in terms of $2N$ SPSs. We anticipate that χ_2^2 will be quite similar to χ_4^2, and that χ_3^2 will be quite similar χ_5^2, because the overcomplete set of $2N$ vectors will not improve or hinder the accuracy of an expansion.

We now proceed to derive expressions for the χ^2s. We start by representing the Gaussian wave packet in the primitive basis.

$$\psi(r) = \sum_{n=1}^{N} \alpha_n y_n(r) \ . \tag{83}$$

We define χ_1^2 as

$$\chi_1^2 = \int_0^{r_f} \left| \psi(r) - \sum_{n=1}^{N} \alpha_n y_n(r) \right|^2 dr \ . \tag{84}$$

Notice that χ_1^2 evaluates the ability of N primitive basis functions to represent the wave packet. We choose α_n to minimize χ_1^2. Setting the derivative with respect to α_n to zero, we obtain

$$\int_0^{r_f} \psi(r) y_m(r) dr = \sum_{n=1}^{N} \alpha_n \int_0^{r_f} y_m(r) y_n(r) dr \ . \tag{85}$$

We define

$$\beta_m = \int_0^{r_f} \psi(r) y_m(r) dr \ , \tag{86}$$

and notice that the overlap matrix appears on the right. Recall that $\underline{Y}^{-1}$ exists. We find that

$$\alpha_m = \sum_{n=1}^{N} \left(\underline{Y}^{-1} \right)_{mn} \beta_n \ . \tag{87}$$

With this we can proceed to calculate χ_1^2 as defined by Eq. (84).

Next we construct χ_2^2. In χ_2^2 we test the ability of the SPSs to recreate $\bar{\alpha}$, the vector of expansion coefficients representing the Gaussian in the primitive basis set. We call this representation of the coefficients $\bar{\tilde{\alpha}}$.

$$\bar{\tilde{\alpha}} = \sum_{m=1}^{N} \gamma_m \bar{c}_m \ . \tag{88}$$

We use this as an occasion to demonstrate the use of the minimal completeness relation (Eq. (81)). We multiply the left side of Eq. (88) by the identity matrix in the form of $\underline{Y}^{-1}\underline{Y}$. We write the resulting expression as

$$\sum_{m=1}^{N} \sum_{n=1}^{N} \bar{c}_m \left(\underline{M}^{-1} \right)_{mn} \bar{c}_n^T \underline{Y} \bar{\tilde{\alpha}} = \sum_{m=1}^{N} \gamma_m \bar{c}_m \ , \tag{89}$$

from which we can pick out

$$\gamma_m = \sum_{n=1}^{N} \left(\underline{M}^{-1} \right)_{mn} \bar{c}_n^T \underline{Y} \bar{\tilde{\alpha}} \ . \tag{90}$$

Inserting γ_m into Eq. (88), we use $\bar{\tilde{\alpha}}$ to calculate χ_2^2 as

$$\chi_2^2 = \sum_{i=1}^{N} |\alpha_i - \tilde{\alpha}_i|^2 \ . \tag{91}$$

χ_3^2 evaluates the ability of the $\tilde{\alpha}_i$s to function as expansion coefficients for the Gaussian in the primitive basis. χ_3^2 has the form of χ_1^2 with the α_i replaced by $\tilde{\alpha}_i$.

$$\chi_3^2 = \int_0^{r_f} \left| \psi(r) - \sum_{j=1}^{N} \left(\sum_{n=1}^{N} \gamma_n c_{jn} \right) y_j(r) \right|^2 dr \ . \tag{92}$$

We also investigate the accuracy of expansions which make use of all $2N$ SPSs. We construct χ_4^2 with a purpose analogous to χ_2^2, and we construct χ_5^2 with a purpose analogous to χ_3^2. To construct χ_4^2 we first expand the coefficients in α in terms of all $2N$ SPSs. Using the completeness relation obeyed by all $2N$ SPSs, we can derive γ_m in

$$\bar{\tilde{\alpha}} = \sum_{m=1}^{2N} \gamma_m \bar{c}_m \ . \tag{93}$$

We use Eq. (62) just as we used Eq. (81). We find

$$\gamma_n = \frac{1}{2} \bar{c}_n^T \underline{Y} \bar{\tilde{\alpha}} \ , \tag{94}$$

which we use to calculate

$$\chi_4^2 = \sum_{i=1}^{N} |\alpha_i - \tilde{\alpha}_i|^2 \ . \tag{95}$$

We calculate χ_5^2 just as χ_3^2 with γ_n now given by Eq. (94).

These five χ^2s were calculated as a function of N, the dimension of the basis. The results are displayed in Table I. Our predictions are confirmed by this numerical analysis. χ_1^2 does in fact converge to an accurate level as N is increased, ensuring that our choice of primitive basis is satisfactory. χ_2^2 and χ_4^2 show that N as well as $2N$ SPSs do indeed span the N dimensional vector space. χ_3^2 and χ_5^2 demonstrate that expanding the wave packet in the basis of SPSs is as accurate as expanding the wave packet in the set of primitive basis functions. It should be acknowledged that χ_2^2 and χ_3^2 presented in the table were calculated utilizing bound and outgoing SPSs. However, experimentation was carried out with all four possible bases of N SPSs; the four cases of N-vector bases demonstrated equivalent performance.

TABLE I: The χ^2's described in Eqs. (83)-(94), as a function of finite-element basis size, N, calculated for the case where $k_0 = 15$ in Eq. (82). χ_1^2 demonstrates convergence to accurate wave-packet reproduction as the number of finite-element basis functions is increased. χ_2^2 and χ_4^2 show the ability of the completeness relations of Eqs. (81) and (62), respectively, to match the unique coefficients of Eq. (87). χ_3^2 and χ_5^2 confirm that these expansions are successful in reproducing the initial wave packet at the level limited by the underlying finite elements. Notation $x[y]$ stands for $x \times 10^y$.

N	χ_1^2	χ_2^2	χ_3^2	χ_4^2	χ_5^2
20	0.89	2.7[−19]	0.89	9.6[−20]	0.89
80	1.5[−3]	1.4[−17]	1.5[−3]	2.2[−19]	1.5[−3]
200	2.0[−7]	4.5[−20]	2.0[−7]	5.3[−21]	2.0[−7]
380	3.0[−11]	7.8[−20]	3.0[−11]	9.8[−21]	3.0[−11]
620	5.5[−14]	4.5[−18]	5.5[−14]	9.9[−19]	5.5[−14]

G. Time evolution

Here we work through the derivation of a time-dependent expansion of the wave packet explored in Sec. III E. Because subsets of N Siegert pseudostates have proven to span our vector space, we seek the time evolution of an expansion across N Siegert pseudostates. We demand representations obey the time-dependent Schrödinger equation (TDSE). It should be explained before the derivation takes place that the result is, in general, incorrect. Numerical investigation indicates the time-dependent expression resulting from demanding Siegert pseudostates obey the TDSE gives accurate evolution if the wave packet being represented has a high kinetic energy expectation value. A more accurate expression for the time evolution of a wave packet will be discussed next. We continue in position representation. The TDSE reads

$$i\frac{\partial}{\partial t}\psi(r,t) = \hat{H}\psi(r,t) \ . \tag{96}$$

We make an ansatz in which the coefficients are time dependent.

$$\psi(r,t) = \sum_{n=1}^{N} \alpha_n(t)\varphi(r) \ . \tag{97}$$

Inserting the ansatz into Eq. (96) and acting with the differential operators inside the summations, we find

$$i\sum_{n=1}^{N}\dot{\alpha}_n(t)\varphi_n(r)=\sum_{n=1}^{N}E_n\varphi_n(r)\ , \tag{98}$$

where $\dot{\alpha}$ indicates differentiation with respect to time, and we have made use of the fact that Siegert pseudostates are eigenstates of the Hamiltonian, that is, they obey Eq. (1). Because everything depends on the same summation index, we can equate the arguments inside the sums.

$$\dot{\alpha}_n(t)=-E_n\alpha_n(t)\ . \tag{99}$$

This differential equation has the familiar solution

$$\alpha_n(t)=\alpha_n(0)e^{-iE_nt}\ . \tag{100}$$

With $\alpha_n(0)$ given by Eq. (77), we can write the time-dependent expansion of a wave packet as

$$\psi(r,t)=\sum_{m=1}^{N}\sum_{n=1}^{N}\left(\underline{M}^{-1}\right)_{mn}\left(\varphi_n|\psi(t=0)\right)e^{-iE_mt}\varphi_m(r)\ . \tag{101}$$

This is a statement of Eq. (79) with standard exponential time evolution multiplying each SPS. As mentioned before, while there are contexts in which this equation provides reasonably accurate time evolution, it can not be considered correct. We must conclude that Siegert pseudostates do not obey the time-dependent Schrödinger equation.

A correct expression for the time evolution of a wave packet in the basis of SPSs can be derived from the Mittag-Leffler partial fraction decomposition of the outgoing wave Green's function represented with respect to Siegert pseudostates [13]. The representation of the Green's function in terms of SPSs was given in [5]. It is derived in [13]. The outgoing-wave Green's function obeys

$$\left(E-\hat{H}\right)G(r,r';k)=\delta(r-r')\ ; \tag{102}$$

$$G(0,r';k)=0\ ; \tag{103}$$

$$\frac{d}{dr}G(r,r';k)\,\big|_{r=r_f}=ikG(r_f,r';k)\ \ . \tag{104}$$

It has the form

$$G(r,r';k)=\sum_{n=1}^{2N}\frac{\varphi_n(r)\varphi_n(r')}{k_n(k-k_n)}\ , \tag{105}$$

where r and r' lie within the interval $[0, r_f]$. With this known, we can obtain $\psi(r,t)$ by

$$\psi(r,t) = \frac{i}{2\pi}\int_{-\infty}^{\infty}\int_{0}^{r_f} e^{-iEt}G(r,r';k)\psi(r',t=0)dr'dE\ . \tag{106}$$

Using the definition of the Green's function, we have

$$\psi(r,t) = \frac{i}{2\pi}\int_{-\infty}^{\infty} e^{-iEt}\sum_{n=1}^{2N}\frac{\varphi_n(r)}{k_n(k-k_n)}\int_{0}^{r_f}\varphi(r')\psi(r',t=0)dr'dE\ , \tag{107}$$

which we write as

$$\psi(r,t) = \sum_{n=1}^{2N}\beta_n(t)\,(\varphi_n|\psi)\,\varphi_n(r)\ , \tag{108}$$

where

$$\beta_n(t) = \frac{i}{2\pi}\int_{-\infty}^{\infty}\frac{e^{-iEt}}{k_n(k-k_n)}dE\ . \tag{109}$$

To solve the integral in Eq. (109), one uses Eq. (8) to write E in terms of k and maps the integral onto the complex k plane. Upon evaluating the integral in Eq. (109) [13], we find that

$$\beta_n(t) = e^{-iV(r_f)t}\times\begin{cases} e^{-ik_n^2t/2} - \frac{1}{2}w\left(e^{i\pi/4}\sqrt{\frac{t}{2}}k_n\right) & \text{for bound or outgoing states} \\ \\ \frac{1}{2}w\left(-e^{i\pi 4}\sqrt{\frac{t}{2}}k_n\right) & \text{for antibound or incoming states} \end{cases}\ , \tag{110}$$

with $w_n(t)$ defined by

$$w(z) = \frac{i}{\pi}\int_{-\infty}^{\infty}\frac{e^{-s^2}}{z-s}ds\ , \tag{111}$$

where $\mathrm{Im}(z) > 0$. The form of a time-dependent expansion into the basis of all $2N$ Siegert pseudostates is given by Eq. (108) with $\beta_n(t)$ given by Eq. (110). The next section contains a numerical evaluation of the accuracy of the two forms of time evolution presented in this section. For more on the Faddeeva function and our method for handling it numerically, see Refs. [16],[15], and [14]. For more on this method for obtaining time evolution, see Ref. [17].

Note that in Eq. (108) all $2N$ SPSs are utilized. We know from Secs. III E and III F that a subset of N SPSs spans the space at any given time, yet this expansion of the outgoing wave Green's function calls upon all $2N$ SPSs. The result of demanding SPSs obey the TDSE, we will show shortly, returns poor accuracy in the case of slow-moving wave packets.

This cannot be due to their inability to span the space, because subsets of N SPSs have proven themselves as bases at $t = 0$. The properties of the vector space itself do not change in time. But as of now, a time-dependent expression for a wave packet in a basis of N Siegert pseudostates eludes us.

H. Testing the accuracy of representations of wave packets in time

In order the evaluate the accuracy of the representation of a wave packet in the basis of Siegert pseudostates as it evolves in time, we need a benchmark for comparison. We again appeal to the square well. There are three reasons why this model potential is appropriate for this context. One, it is a cutoff potential. We can apply the Siegert boundary condition anywhere beyond the discontinuity. Thus, diagonalization of Eq. (23) will lead to solutions with accuracy limited, in principle, by the underlying primitive basis set. Two, the eigensolutions to the square well can be readily derived in analytic form from a consideration of the time-independent Schrödinger equation. We can then expand a wave packet in the basis of the analytic eigenstates and allow each eigenstate to evolve in time in a purely exponential way. This wave packet will serve as our standard for comparison. The third reason the step potential is appropriate in this context is that its discontinuity will give rise to physical reflections. With Siegert pseudostates, we would like to suppress artificial reflections that might arise in computer simulations, but not at the expense of physical reflections. The step potential allows us to assess the ability of the SPSs to capture physical reflections, while allowing the transmitted portion of the wave packet to pass over the barrier. At earlier stages in the development of Siegert pseudostate theory, it was thought that choosing bound and outgoing states as the basis functions for the space would effectively eliminate artificial reflections due to the inability of the outgoing waves to represent the incoming reflections. However, this line of thinking implies that the outgoing SPSs would be incapable of representing the incoming waves of the physical reflections, too. We resort to numerical investigation for more information.

We are comfortable representing a wave packet in the basis of SPSs. We now work toward an expression for a wave packet in terms of analytic eigensolutions to the TISE. Note that standard lower case phi ($\phi(r)$) is used to refer to an analytic solution, whereas cursive lower case phi ($\varphi(r)$) remains the symbol for the position representation of a Siegert pseudostate.

We consider the potential of Eq. (24). The well is called region I, while the region beyond the discontinuity is called region II. In region I, the s-wave TISE in position representation reads

$$\left(-\frac{1}{2}\frac{d^2}{dr^2} - V_0\right)\phi^{(I)}(r) = E\phi^{(I)}(r) \ , \tag{112}$$

The superscript (I) indicates that the function is valid in region I. Upon enforcing vanishing at the origin, Eq. (112) has only one linearly independent solution for a given energy:

$$\phi^{(I)}(r) = A\sin(k^{(I)}r) \ , \tag{113}$$

where

$$k^{(I)} = \sqrt{2(E+V_0)} \ . \tag{114}$$

In region II, the TISE reads

$$-\frac{1}{2}\frac{d^2}{dr^2}\phi^{(II)}(r) = E\phi^{(II)}(r) \ , \tag{115}$$

and the wave number is be related to energy by

$$k^{(II)} = \sqrt{2E} \ . \tag{116}$$

It is useful to anticipate that we will arrive at two types of solutions: bound states and continuum states. The bound states will have negative energy, and thus an imaginary wave number, leading to exponential decay in the space beyond r_0. The bound states will be discrete, so $k, A \to k_n, A_n$. In the continuum $k, A \to k_E, A_E$, and E is a continuous label. For bound states we write the solution in region II as

$$\phi_m^{(II)}(r) = B_m e^{ik_m^{(II)}r} = B_m e^{-\kappa_m^{(II)}r} \ , \tag{117}$$

where

$$\kappa_m^{(II)} = \sqrt{2\left|E_m\right|} \ . \tag{118}$$

For continuum states, we choose to write the solution in region II as

$$\phi_E^{(II)}(r) = B_E\sin(k_E^{(II)}r + \delta) \ , \tag{119}$$

with $k_E^{(II)}$ given by Eq. (116). We will eventually only make use of region I solutions, so our purposes will not necessitate knowledge of δ. Because the TISE relates the potential energy and the second derivative, and because the potential energy is discontinuous but remains

finite at r_0, we know that the second derivative will lose continuity at r_0. Thus, the first derivative will be kinked, but continuous. We can state two boundary conditions valid at the discontinuity.

$$\phi_E^{(I)}(r_0) = \phi_E^{(II)}(r_0) \; ; \tag{120}$$

$$\frac{d}{dr}\phi_E^{(I)}(r)\bigg|_{r=r_0} = \frac{d}{dr}\phi_E^{(II)}(r)\bigg|_{r=r_0} \; . \tag{121}$$

Applying the condition of Eq. (120) to the bound states, we obtain

$$A_n = B_n \frac{e^{-\kappa_n^{(II)} r_0}}{\sin(k_n^{(I)} r_0)} \; . \tag{122}$$

This equation relates the amplitudes of the wave functions in the two regions. If we apply the condition of Eq. (121) and divide the resulting equation by Eq. (122), we arrive at the following transcendental equation.

$$\tan\left(\sqrt{k_n^{(II)2} + 2V_0}\, r_0\right) = \frac{\sqrt{k_n^{(II)2} + 2V_0}}{i k_n^{(II)}} \; , \tag{123}$$

where $k_n^{(II)}$ is related to a negative energy by Eq. (116). Eq. (123) can be solved to obtain the discrete wave numbers $k_n^{(II)}$ of the bound states.

We now seek a relation between the amplitudes of the wave functions in regions I and II applicable to the continuum solutions. If we apply Eqs. (120) and (121) to the solutions in Eqs. (113) and (119) we arrive at the two expressions

$$A_E \sin(k_E^{(I)} r_0) = B_E \sin(k_E^{(II)} r_0 + \delta) \; , \tag{124}$$

and

$$A_E \cos(k_E^{(I)} r_0) = \frac{k_E^{(II)}}{k_E^{(I)}} B_E \cos(k_E^{(II)} r_0 + \delta) \; . \tag{125}$$

If we now add Eqs. (124) and (125) in quadrature, we obtain

$$A_E^2 = B_E^2 \left[\sin^2(k_E^{(II)} r_0 + \delta) + \left(\frac{k_E^{(II)}}{k_E^{(I)}}\right)^2 \cos^2(k_E^{(II)} r_0 + \delta) \right] \; . \tag{126}$$

We would like to eliminate δ from the expression. We divide Eq. (124) by Eq. (125).

$$\tan(k_E^{(I)} r_0) = \frac{k_E^{(I)}}{k_E^{(II)}} \tan(k_E^{(II)} r_0 + \delta) \; . \tag{127}$$

Making use of the relation

$$\cos^2(x) = \frac{1}{1+\tan^2(x)} \ , \tag{128}$$

we discover

$$\cos^2(k_E^{(II)} r_0 + \delta) = \frac{1}{1+\left(\frac{k_E^{(II)}}{k_E^{(I)}}\right)^2 \tan^2(k_E^{(I)} r_0)} \ . \tag{129}$$

With a few algebraic manipulations, we can write

$$\sin^2(k_E^{(II)} r_0 + \delta) + \left(\frac{k_E^{(II)}}{k_E^{(I)}}\right)^2 \cos^2(k_E^{(II)} r_0 + \delta) \tag{130}$$

$$= \left[\frac{(k_E^{(II)}/k_E^{(I)})^2}{\cos^2(k_E^{(I)} r_0) + (k_E^{(II)}/k_E^{(I)})^2 \sin^2(k_E^{(I)} r_0)}\right]^{1/2} \ .$$

Thus,

$$A_E = B_E \left[\frac{(k_E^{(II)}/k_E^{(I)})^2}{\cos(k_E^{(I)} r_0) + (k_E^{(II)}/k_E^{(I)})^2 \sin(k_E^{(I)} r_0)}\right]^{1/2} \ . \tag{131}$$

Because $k_E^{(I)}$ and $k_E^{(II)}$ depend on energy, we have an energy-dependent expression relating the normalization constants A_E and B_E. Note that this expression is independent of the phase shift, δ.

In this case, as well as in the case of the bound states, we still must find either A_E or B_E as a function of energy. We anticipate this resulting from the demand that our solutions be energy normalized. We see where this demand enters if we express an arbitrary wave packet in the basis of analytic eigenstates of the square-well Hamiltonian.

$$\psi(r) = \sum_n C_n \phi_n(r) + \int_0^\infty C_E \phi_E(r) dE \ . \tag{132}$$

In this expression the sum is over the discrete bound states, and the integration is over the continuum of positive energy states. To find the coefficients C_n and C_E, we make use of the orthogonality of eigenstates of the Hamiltonian.

$$C_n = \int_0^{r_0} \phi_n^{(I)*}(r)\psi(r)dr + \int_{r_0}^\infty \phi_n^{(II)*}(r)\psi(r)dr \ , \tag{133}$$

if

$$\int_0^{r_0} \phi_m^{(I)*}(r)\phi_n^{(I)}(r)dr + \int_{r_0}^\infty \phi_m^{(II)*}(r)\phi_n^{(II)}(r)dr = \delta_{mn} \ , \tag{134}$$

and

$$C_E = \int_0^{r_0} \phi_E^{(I)*}(r)\psi(r)dr + \int_{r_0}^\infty \phi_E^{(II)*}(r)\psi(r)dr \ , \tag{135}$$

if

$$\int_0^{r_0} \phi_E^{(I)*}(r)\phi_{E'}^{(II)}(r)dr + \int_{r_0}^{\infty} \phi_E^{(II)*}(r)\phi_{E'}^{(II)}(r)dr = \delta(E-E') \ . \tag{136}$$

Eq. (134) is easily enforced. Performing the integration, we find

$$A_n = \left[\frac{r_0}{2} - \frac{\sin(2k_E^{(I)}r_0)}{4k_E^{(I)}} + \frac{\sin^2(k_E^{(I)}r_0)}{2k_E^{(II)}}\right]^{-1/2} \ . \tag{137}$$

Enforcing Eq. (136) is more sophisticated. The equation reads

$$\begin{aligned} & A_E^2 \int_0^{r_0} \sin(k_E^{(I)}r)\sin(k_{E'}^{(I)}r)dr \\ +B_E^2 & \int_{r_0}^{\infty} \sin(k_E^{(II)}r+\delta)\sin(k_{E'}^{(II)}r+\delta)dr = \delta(E-E') \ . \end{aligned} \tag{138}$$

The first integral will vanish in comparison to the delta function on the right hand side. We write the sines in the second integral in their exponential form.

$$\begin{aligned} & \int_{r_0}^{\infty} e^{i(k_E^{(II)}+k_{E'}^{(II)})r-\epsilon r}dr + \int_{r_0}^{\infty} e^{-i(k_E^{(II)}+k_{E'}^{(II)})r-\epsilon r}dr \\ & - \int_{r_0}^{\infty} e^{i(k_E^{(II)}-k_{E'}^{(II)})r-\epsilon r}dr - \int_{r_0}^{\infty} e^{i(k_{E'}^{(II)}+k_E^{(II)})r-\epsilon r}dr \\ & = \frac{4}{B_E^2}\delta(E-E') \ . \end{aligned} \tag{139}$$

The ϵr argument has been included in the exponential of each integrand to provide convergence at $r \to \infty$. Upon integrating, we find

$$\begin{aligned} & \frac{-ie^{i(k_E^{(II)}+k_{E'}^{(II)})r_0}}{i\epsilon - (k_E^{(II)}+k_{E'}^{(II)})} + \frac{ie^{-i(k_E^{(II)}+k_{E'}^{(II)})r_0}}{i\epsilon - (k_E^{(II)}+k_{E'}^{(II)})} \\ & + \frac{ie^{i(k_E^{(II)}-k_{E'}^{(II)})r_0}}{i\epsilon + (k_{E'}^{(II)}-k_E^{(II)})} + \frac{ie^{i(k_{E'}^{(II)}-k_E^{(II)})r_0}}{i\epsilon + (k_E^{(II)}-k_{E'}^{(II)})} \\ & = \frac{4}{B_E^2}\delta(E-E') \ . \end{aligned} \tag{140}$$

We can make use of the formula

$$\frac{1}{x+i\epsilon} = Pr\frac{1}{x} - i\pi\delta(x) \ , \tag{141}$$

where $Pr\frac{1}{x}$ refers to the principal value integral of $\frac{1}{x}$. We acknowledge that all the principle value integrals which arise vanish, as do the delta functions wherein $k_E^{(II)}$ and $k_{E'}^{(II)}$ have the same sign. We are left with

$$\frac{B_E^2}{2}\pi\delta(\sqrt{2E}-\sqrt{2E'}) = \delta(E-E') \ . \tag{142}$$

We now make use of the expression

$$\delta(f(x)) = \sum_i \frac{1}{\left|\frac{d}{dx}f(x_i)\right|}\delta(x - x_i) \ , \tag{143}$$

where the index i runs over the zeroes of $f(x)$. We encounter one zero when $E = E'$. We obtain

$$\delta(\sqrt{2E} - \sqrt{2E'}) = \sqrt{2E'}\delta(E - E') \ . \tag{144}$$

Integrating across the identical delta functions, we find

$$B_E = \left(\frac{2}{\pi\sqrt{2E}}\right)^{1/2} \ . \tag{145}$$

From this, A_E is also accessible. Observe that B_E becomes imaginary when the energy becomes negative. For negative-energy solutions we must use the discretized normalization coefficients of Eq. (137).

This exercise in energy normalization has provided us with all of the energy-dependent normalization coefficients we need to have complete solutions in region I of this square-well model. An arbitrary wave packet can now be expressed in the basis of analytic eigenfunctions according to Eq. (132). A complete time-dependent expression has the form

$$\psi(r,t) = \sum_n C_n\phi_n(r)e^{-iE_nt} + \int_0^\infty C_E\phi_E(r)e^{-iEt}dE \ , \tag{146}$$

where C_n and C_E are given by Eqs. (133) and (135) respectively.

With this complete analytic representation of a wave packet in time derived directly from standard quantum mechanics, we can now test the accuracy of a wave packet evolving in time expanded in the basis of Siegert pseudostates. We qualify our standard for comparison (Eq. (146)) by confirming that it represents the Gaussian wave packet of study (Eq. (82)) to machine precision at $t = 0$. We then proceed to compare the wave packet in the SPS basis with the wave packet in the analytical basis[32], confident that any discrepancy is due to error on the part of the Siegert pseudostates.

We can expand in the basis of SPSs in two ways: by making use of N SPSs and assuming each evolves in time according to the standard exponential phase factor (Eq. (101)), or by making use of all $2N$ SPSs and utilizing the time-dependent expansion coefficients of Eq. (110). We consider both expressions for time evolution and treat two cases—one with a fast moving wave packet, sufficient kinetic energy to overcome the discontinuity with little

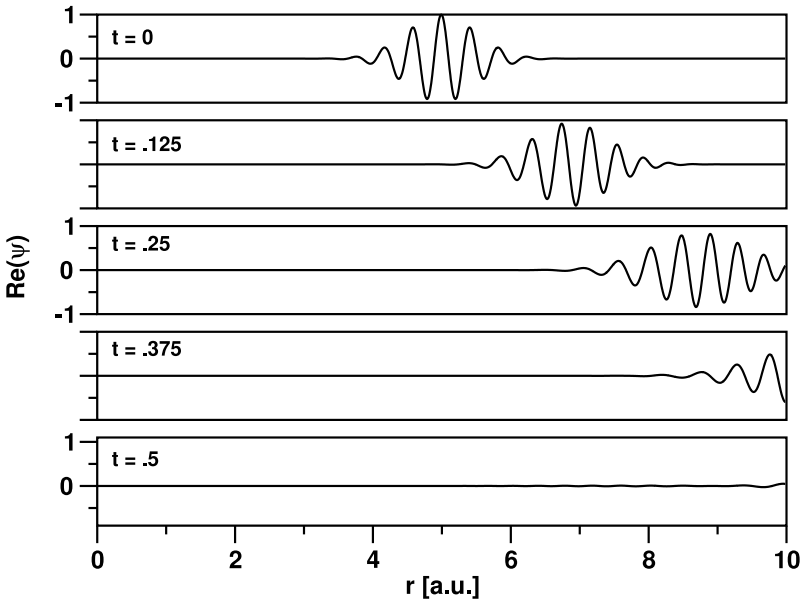

FIG. 10: Time evolution of the wave packet described at $t = 0$ by Eq. (82); $k_0 = 15$. In the r interval between 0 and 10, the potential is constant [$V_0 = 5$ and $r_0 = 10$ in Eq. (24)].

physical reflection, and one with a slower wave packet, which experiences significant physical reflection. The wave packets are shown in Figs. 10 and 11. We modify χ_3^2 and χ_5^2 (Sec. III F) to include time dependence. We refer to the modified forms of the expressions as $\chi_3^2(t)$ and $\chi_5^2(t)$. Explicitly,

$$\chi_3^2(t) = \int_0^{r_f} \left| \psi(r,t) - \sum_{n=1}^{N} \gamma_n \varphi_n(r) e^{-iE_n t} \right|^2 dr \ ; \tag{147}$$

$$\chi_5^2(t) = \int_0^{r_f} \left| \psi(r,t) - \sum_{n=1}^{2N} \beta_n (\varphi_n | \psi_{t=0}) \varphi_n(r) \right|^2 dr \ . \tag{148}$$

Note that in these expressions, $\psi(r,t)$ is the wave packet expanded in terms of the analytical solutions to the step potential (Eq. (146)). These two χ^2s were calculated for various times with the parameters $V_0 = 5$, $r_0 = r_f = 10$, and for the two k_0-values $k_0 = 5$ and $k_0 = 15$. The results are shown in Tables II and III. Table II reveals that for the fast-moving wave packet, both forms provide satisfactory time evolution. But Table III shows that for the slower wave packet, only the expression making use of all $2N$ SPSs provides satisfactory agreement with the analytical expression. From this we conclude that exponential time

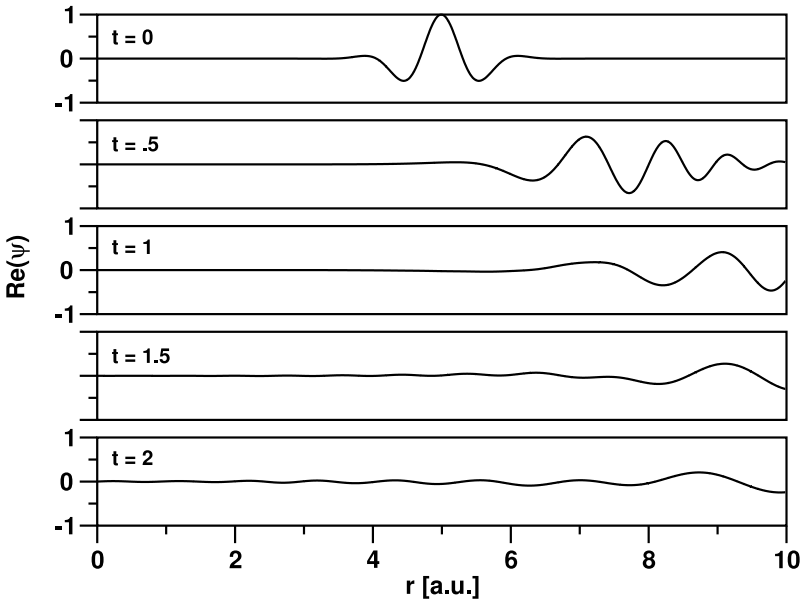

FIG. 11: The same parameters as in Fig. 10, but with $k_0 = 5$. Notice that there are significant physical reflections as soon as the wave packet hits the discontinuity at $r = r_0$.

evolution is, in general, incorrect in the context of Siegert pseudostates. We also notice that, in both the case with significant physical reflection and near-complete transmission of the wave packet, the time evolution of Eq. (108) returns a highly accurate representation of the wave packet, confirming that SPSs are capable of capturing physical reflections without introducing artificial reflections at the boundary of the volume considered in the numerical treatment.

An interesting point to mention regards the claim that SPSs do not introduce artificial reflections when the subset of bound and outgoing states are utilized as a basis because the outgoing waves are incapable of representing incoming wave character. The quality performance demonstrated by all $2N$ SPSs sheds no light on this issue. However, though the fast wave packet in Fig. 10 had enough kinetic energy to pass over the discontinuity with little physical reflection, one is still able to see (Fig. 10) the occurrence of reflections emanating from the step toward the origin. The magnitude of these reflections is orders of magnitude larger than the errors indicated by the χ^2s. Also, simulations in which only bound and outgoing Siegert pseudostates were utilized as basis functions for representing

TABLE II: The time-dependent χ^2's discussed in Sec. III H for the case of the fast-moving wave packet ($k_0 = 15$; see Fig. 10). $\chi_3^2(t)$ measures the quality of exponential time evolution. For $\chi_3^2(t)$, the wave packet is expanded in a basis of bound and outgoing Siegert pseudostates [Eq. (101)]. $\chi_5^2(t)$ refers to nonexponential time evolution using all $2N$ Siegert pseudostates [Eqs. (108), (110)]. $\| \psi(t) \|^2$ is defined by $\| \psi(t) \|^2 = \int_0^{r_f} |\psi(r,t)|^2 \, dr$. The information in this table confirms that both expansions are accurate in describing the motion of a higher-energy particle.

t [a.u.]	$\chi_3^2(t)/ \| \psi(t) \|^2$	$\chi_5^2(t)/ \| \psi(t) \|^2$
0	6.2×10^{-14}	6.2×10^{-14}
0.125	1.4×10^{-13}	1.4×10^{-13}
0.25	2.2×10^{-13}	2.2×10^{-13}
0.375	1.5×10^{-12}	1.5×10^{-12}
0.5	1.9×10^{-9}	1.9×10^{-9}

TABLE III: The case of the slow-moving wave packet ($k_0 = 5$; see Fig. 11). The $\chi^2(t)$s measure the same quantities as in Table II. For both forms of expansion coefficients the accuracy at $t = 0$ is only limited by the finite-element basis set. For $t > 0$, $\chi_5^2(t)$ is many orders of magnitude smaller than $\chi_3^2(t)$, showing that, for this case, accurate time evolution is given by the expansion of Eq. (108) using the nonexponential time-evolution coefficients in Eq. (110).

t [a.u.]	$\chi_3^2(t)/ \| \psi(t) \|^2$	$\chi_5^2(t)/ \| \psi(t) \|^2$
0	2.9×10^{-16}	2.9×10^{-16}
0.5	6.2×10^{-6}	5.3×10^{-16}
1	5.5×10^{-5}	2.2×10^{-15}
1.5	4.4×10^{-4}	2.4×10^{-14}
2	1.2×10^{-3}	2.3×10^{-13}

both the slow and the fast wave packets showed behavior nearly identical to simulations with $2N$ SPSs. Discrepancies were not visible to the eye. In these simulations, the basis of N SPSs comprised of bound and outgoing states displayed lovely reflections, demonstrating the ability of bound and outgoing waves to, when superposed, model incoming wave character. The fact that their demonstration was not accurate beyond three decimal places must be

attributed to their obeying an alternate form of time evolution, not to their inability to represent incoming waves.

With issues of completeness and time evolution within the formalism of Siegert pseudostates understood, we turn our attention to the treatment of a two-channel model within the formalism of Siegert pseudostates.

IV. TWO COUPLED CHANNELS

We now advance the theory of Siegert pseudostates to treat coupled channels. Before diving into a specific case, it will be useful to develop the underlying concepts of multi-channel interactions.

A. Coupled-channel physics

Many physical interactions involve more than one channel [1] [2] [7]. Multiple channels arise when a Hamiltonian involves several degrees of freedom. For simplicity, let us consider a Hamiltonian with two degrees of freedom. Such a problem is usually solved by treating one degree of freedom as a parameter, that is, keeping it fixed at a specific value. With one degree of freedom set to have a particular value, the Hamiltonian is then diagonalized. The result may be a discrete number of energy states. Next, one changes the value of the degree of freedom being treated as a parameter and diagonalizes the Hamiltonian again to find new energy levels. Repeating this procedure will lead to energy curves modeling the results one would obtain if they were able to completely diagonalize the Hamiltonian with two degrees of freedom. As an example, consider a Hamiltonian wherein the two degrees of freedom are the distance between two particles, labeled by r, and the angular momentum, labeled by l. For a chosen value of r, diagonalization of the Hamiltonian will result in several possible energies corresponding to different values of the quantum number l. Suppose we are only interested in the lowest four. We note these values, increase r by a small amount, and diagonalize the Hamiltonian again. We repeat this procedure until we have covered the region of space that concerns us. The results of such a procedure may be similar to the curves shown in Fig. 12. Each curve corresponds to a channel. While some of the curves have wells, some are more shallow. The wells may house bound states, while the flatter

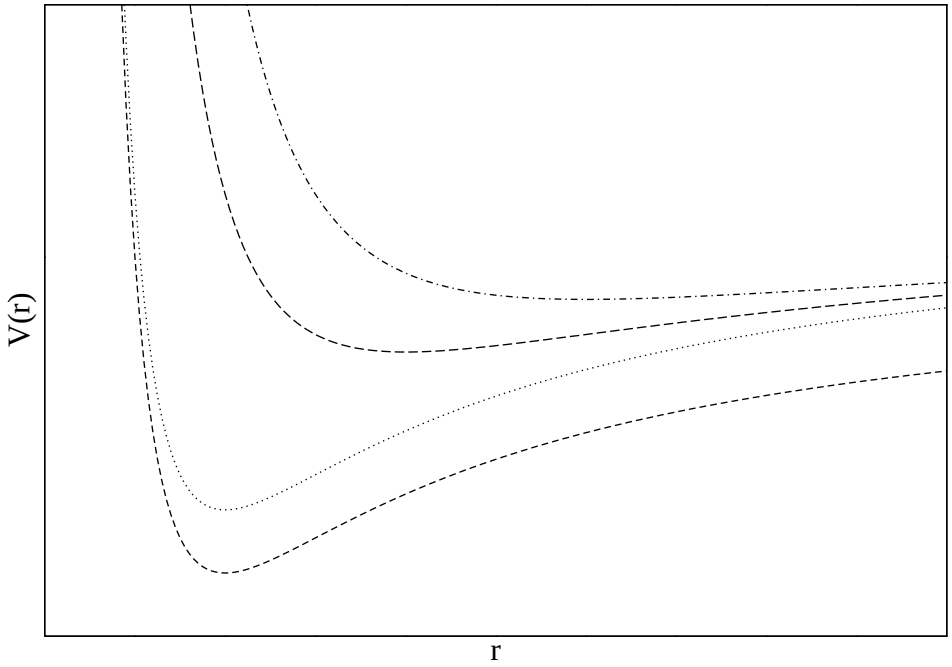

FIG. 12: An example of multiple potential energy curves corresponding to multiple channels a system may experience. Units are arbitrary. Some of the curves may hold bound states, while some may be too shallow.

curves may not. Exciting a particle from a bound state in a channel with a well to a channel without bound states can result in dissociation of the two-particle bound state.

B. The multi-channel Hamiltonian

If it is now somewhat clear what is meant by multi-channel interactions, there is still ambiguity in the term coupled-channels. If channels are uncoupled, a particle experiencing one channnel knows nothing of other channels, and cannot transition between channels. Eigenstates of an uncoupled multi-channel Hamiltonian are contained in a vector whose elements are the independent-channel eigenstates, and whose length is the number of channels. In the case of coupled channels, a particle more localized in one channel may "leak" into other channels. Eigenstates of a coupled multi-channel Hamiltonian can have components

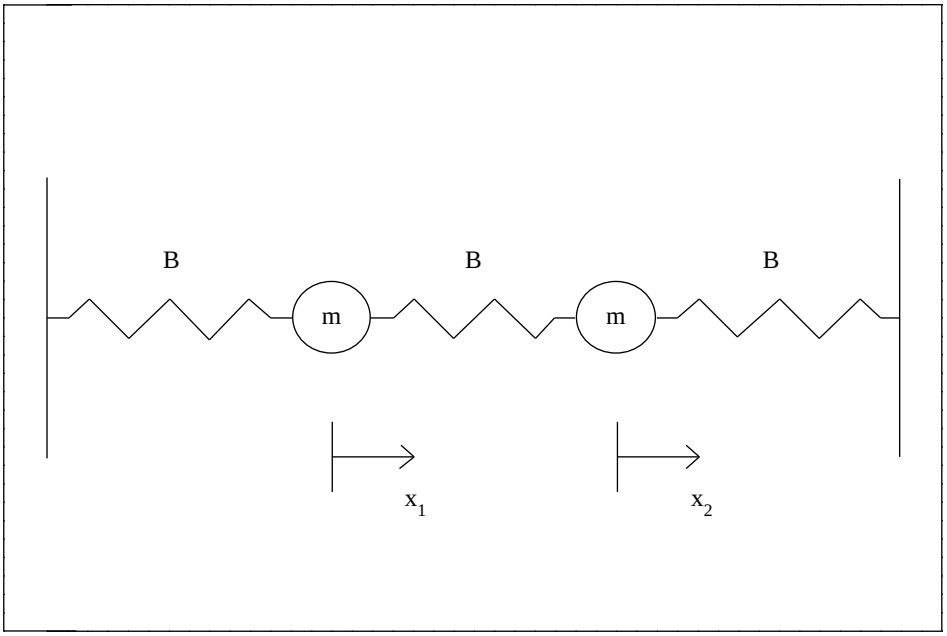

FIG. 13: Two coupled oscillators, each of mass m attached to each other and to fixed walls by springs of Hooke's law constant B. Motion is confined to one dimension.

in multiple channels. An N-channel Hamiltonian has the form

$$\underline{\hat{H}} = \begin{pmatrix} \hat{H}_1 & \hat{V}_{12} & \hat{V}_{13} & \cdots & \hat{V}_{1N} \\ \hat{V}_{21} & \hat{H}_2 & \hat{V}_{23} & \cdots & \hat{V}_{2N} \\ \hat{V}_{31} & \hat{V}_{32} & \hat{H}_3 & & \\ \vdots & \vdots & & \ddots & \\ \hat{V}_{N1} & \hat{V}_{N2} & & & \hat{H}_N \end{pmatrix} , \tag{149}$$

where the diagonal elements are the independent-channel Hamiltonians. In standard units,

$$\hat{H}_i = -\frac{\hbar^2}{2m}\nabla^2 + \hat{V}_i(\bar{r}) \ . \tag{150}$$

The off diagonal elements $\hat{V}_{ij}$ represent coupling between channels. Notice that if all $\hat{V}_{ij} = 0$, the matrix is diagonal, and complete eigensolutions are simply the list of eigensolutions to the uncoupled-channel Hamiltonians. If $\hat{V}_{ij} \neq 0$ for some or all i, j, the Hamiltonian must be diagonalized, which effectively mixes eigenstates between channels.

C. Classical coupled oscillators

To further illustrate the phenomenon of coupling, we visit the example of classical coupled harmonic oscillators. The physical scenario we consider is shown in Fig. 13. The masses are attached to each other and to the walls by springs. For simplicity, we have chosen all spring constants to be the same (B), and all masses to be the same (m). Because the two masses are connected by a spring, something that can store potential energy, the motion of each influences the other in an interesting way. It is in this sense that they are coupled. We define the motion of each mass by a coordinate x_i which measures its displacement from equilibrium. If we consider the vector

$$\bar{a}_1 = \begin{pmatrix} 1 \\ 0 \end{pmatrix} \ , \tag{151}$$

corresponding to moving the first mass by one unit, and the vector

$$\bar{a}_2 = \begin{pmatrix} 0 \\ 1 \end{pmatrix} \ , \tag{152}$$

corresponding to moving the second mass by one unit, we can write any displacement of the two masses as a linear combination of these two vectors.

$$\begin{pmatrix} x_1 \\ x_2 \end{pmatrix}_c = x_1\bar{a}_1 + x_2\bar{a}_2 \ . \tag{153}$$

The subscript c indicates that the vector contains information with respect to the basis in which motion is coupled. x_1 and x_2 describe the displacement of each mass at a given time. A change in x_1 necessarily means a change in x_2. This is what it means to be coupled. The vectors $\bar{a}_1$ and $\bar{a}_2$ span the space of all possible displacements of the masses in coordinates that are easy to understand physically. But in these coordinates we do not see differential equations that are easy to solve. Still, we can derive the equations of motion that they do obey, and represent those equations in an uncoupled basis. The Lagrangian for the system reads

$$L = \frac{1}{2}m\left(\dot{x}_1^2 + \dot{x}_2^2\right) - \frac{1}{2}B\left[x_1^2 + x_2^2 + (x_1 - x_2)^2\right] \ . \tag{154}$$

The associated equations of motion are

$$\ddot{x}_1 = -\frac{B}{m}(2x_1 - x_2) \ , \tag{155}$$

and

$$\ddot{x}_2 = -\frac{B}{m}(2x_2 - x_1) \ . \tag{156}$$

We see that these equations are coupled; x_2 appears in the equation of motion for x_1 and vice versa. We can capture Eqs. (155) and (156) in a 2×2 matrix equation.

$$\begin{pmatrix} \ddot{x}_1 \\ \ddot{x}_2 \end{pmatrix}_c = \begin{pmatrix} -\frac{2B}{m} & \frac{B}{m} \\ \frac{B}{m} & -\frac{2B}{m} \end{pmatrix} \begin{pmatrix} x_1 \\ x_2 \end{pmatrix}_c \ . \tag{157}$$

Notice the off-diagonal coupling occurring in the matrix. We must move to a basis in which the matrix relating each coordinate to its second derivative is diagonal, and the equations of motion are uncoupled. We will refer to solutions in the uncoupled representation as eigensolutions. Each will be associated with a particular type of motion, called an eigenmode. The natural frequency of oscillation of an eigenmode is its eigenfrequency.

We proceed to find the eigenmodes, which will tell us about the motion of the masses. The task is to find a set of basis vectors for the space of all possible configurations of the system that diagonalizes the matrix of Eq. (157). The matrix is real, and it is symmetric because we have considered identical masses and identical springs. These two statements ensure that the matrix is Hermitian. Note that we diagonalize the matrix by a similarity transformation, just as we did $\underline{B}$ in Sec. III E. The basis which diagonalizes a Hermitian matrix is the basis composed of the eigenvectors of the matrix. We define the matrix

$$\underline{W} = \begin{pmatrix} \frac{-2B}{m} & \frac{B}{m} \\ \frac{B}{m} & \frac{-2B}{m} \end{pmatrix} \ , \tag{158}$$

and note that

$$\underline{A}^T \underline{W} \underline{A} = \begin{pmatrix} -\omega_1^2 & 0 \\ 0 & -\omega_2^2 \end{pmatrix} \ , \tag{159}$$

where $-\omega_1^2$ and $-\omega_2^2$ are the eigenvalues of $\underline{W}$, and $\underline{A}$ the matrix of composed of the eigenvectors of $\underline{W}$. Upon diagonalization of $\underline{W}$, we find two eigenvectors and their eigenvalues:

$$\bar{A}_1 = \frac{1}{\sqrt{2}} \begin{pmatrix} 1 \\ 1 \end{pmatrix} \ , \tag{160}$$

associated with

$$\omega_1^2 = -\frac{B}{m} \ , \tag{161}$$

and

$$\bar{A}_2 = \frac{1}{\sqrt{2}} \begin{pmatrix} 1 \\ -1 \end{pmatrix} \ , \tag{162}$$

associated with

$$\omega_2^2 = -\frac{3B}{m} \ . \tag{163}$$

The vectors $\bar{A}_1$ and $\bar{A}_2$ are the basis vectors corresponding to the eigenmodes of oscillation, and ω_1 and ω_2 are the associated eigenfrequencies. In this basis, Eq. (157) takes the form

$$\begin{pmatrix} \ddot{y}_1 \\ \ddot{y}_2 \end{pmatrix}_u = \begin{pmatrix} -\omega_1^2 & 0 \\ 0 & -\omega_2^2 \end{pmatrix} \begin{pmatrix} y_1 \\ y_2 \end{pmatrix}_u \ . \tag{164}$$

We refer to the matrix in Eq. (164) as $\underline{\omega}^2$, and y_1 and y_2 are the coordinates of motion in the eigenrepresentation, that is

$$\begin{pmatrix} y_1 \\ y_2 \end{pmatrix}_u = y_1 \bar{A}_1 + y_2 \bar{A}_2 \ . \tag{165}$$

The subscript u emphasizes that the vectors are represented in the uncoupled basis. Eq. (164) leads to two uncoupled differential equations describing motion in the eigenrepresentation. The solutions to the two equations are the eigensolutions. We will not seek them here, but comment that they are essentially sines, which, when differentiated twice will bring out a constant squared and a negative sign. The constant will be the sine's frequency. It is for this reason that we write the diagonal elements of $\underline{\omega}^2$ as constants squared. These are the eigenfrequencies of the model.

We would like to express the basis vectors of the eigenrepresentation as linear combinations of the basis vectors of the coupled representation in order to get a qualitative understanding of the motion. We can write

$$\bar{A}_1 = \frac{1}{\sqrt{2}} \left(\bar{a}_1 + \bar{a}_2 \right) \ , \tag{166}$$

and

$$\bar{A}_2 = \frac{1}{\sqrt{2}} \left(\bar{a}_1 - \bar{a}_2 \right) \ . \tag{167}$$

Notice the occurrence of a basis vector which is symmetric and one which is antisymmetric under exchange of particle labels.

We can now understand the motion physically, that is, interpret the eigenmodes $\bar{A}_1$ and $\bar{A}_2$. The mode of oscillation expressed by $\bar{A}_1$ corresponds to the two particles moving in

unison, and the mode expressed by $\bar{A}_2$ corresponds to motion out of phase by π. These two types of motion are completely orthogonal and do not influence each other; these are uncoupled modes. Eigenmode $\bar{A}_1$ corresponds to motion with angular eigenfrequency $\sqrt{B/m}$, whereas eigenmode $\bar{A}_2$ has frequency $\sqrt{3B/m}$, indicating higher energy oscillations. Any physical motion will be a superposition of these two modes, analogous to a particle having probability in several channels.

There are many lessons about coupled-channel physics to be learned from this example of coupled oscillators. We began with a matrix equation in which the matrix had off-diagonal elements corresponding to coupling. We moved the equation to a basis in which the matrix was diagonal. In this representation we had access to whatever information we desired regarding the problem. In this example, we identified the two present independent modes of oscillation, noted their respective eigenfrequencies, and concluded that any physical state will be a superposition of these modes. We then moved back to the basis in which the eigenmodes were easily interpreted. Almost nothing changes conceptually or mathematically if we go from coupled oscillators to coupled channels. We diagonalize the coupled-channel matrix equation to find a basis where the channels are uncoupled. We find answers to our questions in this representation, then move back to the original basis, if desired, to make sense of the findings. We observe the same phenomenon of channels having different energies, and of physical states with components in several channels.

D. Siegert pseudostates in two coupled channels

We proceed with the derivation of a generalized eigenvalue problem analogous to Eq. (23), but in the presence of two-channels [18]. In a two-channel case, the Hamiltonian of Eq. (149) becomes a 2×2 matrix. We write it as

$$\underline{\hat{H}} = \begin{pmatrix} \hat{H}_o & \hat{V}_{oc} \\ \hat{V}_{co} & \hat{H}_c \end{pmatrix} . \tag{168}$$

The subscripts refer to open and closed channels. A channel is said to be open if the particle experiencing it has sufficient energy to escape to an asymptotic region. If the kinetic energy of the body experiencing the channel is less than the asymptotic potential energy of that channel, the body behaves as if it were bound in that channel; we refer to the channel as

closed. We choose to construct our model with one open and one closed channel, though the derivation differs little for two open channels. As elements of the Hamiltonian we have

$$\hat{H}_o = -\frac{1}{2}\frac{d^2}{dr^2} + \hat{V}_o(r) \ , \tag{169}$$

$$\hat{H}_c = -\frac{1}{2}\frac{d^2}{dr^2} + \hat{V}_c(r) \ , \tag{170}$$

and off diagonal elements representing (possibly position-dependent) coupling between the two channels. Our ansatz is a 2-element vector wherein each element is an expansion into the chosen primitive basis set.

$$\varphi(r) = \begin{pmatrix} \sum_{n=1}^{N} c_n^{(o)} y_n(r) \\ \sum_{n=1}^{M} c_n^{(c)} y_n(r) \end{pmatrix} \ . \tag{171}$$

The top summation considers the open channel, the bottom the closed. We utilize superscripts in this derivation to refer to separate channels, not separate regions in space. We anticipate that the portion of the wave function which is in the closed channel will decay for large r. There will be a radius r_f for which the wave function in the closed channel is zero. We choose r_f sufficiently large so that the wave functions bound by the closed channel will have decayed to zero. One must be careful in later uses of eigenstates to not utilize those eigenstates whose energies are high enough that they would not lead to sufficient decay by r_f. Understanding this concern, we proceed.

In practical numerical calculations, the two channels may necessitate different numbers of basis functions. For the sake of generality, we allow the expansion in the open channel to have a different number of terms than the expansion in the closed channel.

We seek the matrix elements of the TISE, Eq. (1).

$$(y_m(r)y_m(r)) \begin{pmatrix} \hat{H}_o & \hat{V}_{oc} \\ \hat{V}_{co} & \hat{H}_c \end{pmatrix} \begin{pmatrix} \sum_{n=1}^{N} c_n^{(o)} y_n(r) \\ \sum_{n=1}^{M} c_n^{(c)} y_n(r) \end{pmatrix} = E\,(y_m(r)y_m(r)) \begin{pmatrix} \sum_{n=1}^{N} c_n^{(o)} y_n(r) \\ \sum_{n=1}^{M} c_n^{(c)} y_n(r) \end{pmatrix} \ . \tag{172}$$

Carrying this multiplication through and integrating over the reaction volume, we find

$$\begin{aligned} & \sum_{n=1}^{N} c_n^{(o)} \int_0^{r_f} y_m(r)\hat{H}_o y_n(r)dr + \sum_{n=1}^{N} c_n^{(o)} \int_0^{r_f} y_m(r)\hat{V}_{co} y_n(r)dr \qquad (173) \\ + & \sum_{n=1}^{M} c_n^{(c)} \int_0^{r_f} y_m(r)\hat{H}_c y_n(r)dr + \sum_{n=1}^{M} c_n^{(c)} \int_0^{r_f} y_m(r)\hat{V}_{oc} y_n(r)dr \\ = & E\left(\sum_{n=1}^{N} c_n^{(o)} \int_0^{r_f} y_m(r) y_n(r)dr + \sum_{n=1}^{M} c_n^{(c)} \int_0^{r_f} y_m(r) y_n(r)dr \right) . \end{aligned}$$

We can immediately define several matrices by their elements.

$$V_{mn}^{(co)} = 2 \int_0^{r_f} y_m(r)\hat{V}_{co} y_n(r)dr \; . \qquad (174)$$

The factor of two comes from a multiplication of the entire problem by two in order to compensate for the 1/2 introduced by the kinetic energy operator. $\underline{V}^{(co)}$ is an $M \times N$ matrix. If we make the assumption that the Hamiltonian is Hermitian, $\underline{V}^{(oc)} = \underline{V}^{(co)T}$, and $\underline{V}^{(oc)}$ is an $N \times M$ matrix.

The overlap matrix in the open channel is an $N \times N$ matrix. Here we will use the factor of two to cancel the 1/2 introduced when relating energy to momentum.

$$Y_{mn}^{(o)} = \int_0^{r_f} y_m(r) y_n(r)dr \; . \qquad (175)$$

The overlap matrix in the closed channel is an $M \times M$ matrix.

$$Y_{mn}^{(c)} = \int_0^{r_f} y_m(r) y_n(r)dr \; . \qquad (176)$$

To identify the matrix elements of the energy operators, we consider the integrals resulting from the diagonal elements of the Hamiltonian operator in more detail. In the open channel, we obtain a solution very similar to the one-channel case. Applying the same technique of partial integration that we employed in the one-channel derivation and enforcing the boundary conditions of Eqs. (11) and (12), we obtain

$$\tilde{H}_{mn}^{(o)} = \int_0^{r_f} \frac{d}{dr} y_m(r) \frac{d}{dr} y_n(r)dr + 2 \int_0^{r_f} y_m(r)\hat{V}_o(r) y_n(r)dr \; , \qquad (177)$$

and

$$L_{mn}^{(o)} = y_m(r_f) y_n(r_f) \; . \qquad (178)$$

Both $\underline{\tilde{H}}^{(o)}$ and $\underline{L}^{(o)}$ are $N \times N$ matrices.

In the closed channel, integrating by parts leads to a term that vanishes at the origin, and a term that vanishes at the boundary. We are left with

$$\tilde{H}^{(c)}_{mn} = \int_0^{r_f} \frac{d}{dr} y_m(r) \frac{d}{dr} y_n(r) dr + 2 \int_0^{r_f} y_m(r) \hat{V}_c(r) y_n(r) dr \ , \tag{179}$$

which is an $M \times M$ matrix. It is the same $\underline{\tilde{H}}$ we have been dealing with, but it is not accompanied by a surface matrix. It makes physical sense that if we choose r_f sufficiently large, there will be no surface term in the closed channel.

We can now write our equation in matrix form. We call the vector of expansion coefficients for the open channel $\bar{c}^{(o)}$ and the vector of expansion coefficients for the closed channel $\bar{c}^{(c)}$. Because we are dealing with matrices of different dimensions, we must be careful to write two equations—one where matrix-vector multiplication leads to vectors of length M, and one where vectors of length N are obtained. These will be the coupled equations making up the matrix equation that we must diagonalize. In the closed channel we have

$$\left[\underline{\tilde{H}}^{(c)} + \underline{V}^{(oc)}\right] \bar{c}^{(c)} = k^2 \underline{Y} \bar{c}^{(c)} \ , \tag{180}$$

and in the open channel

$$\left[\underline{\tilde{H}}^{(o)} + \underline{V}^{(co)} - ik\underline{L}^{(o)}\right] \bar{c}^{(o)} = k^2 \underline{Y}^{(o)} \bar{c}^{(o)} \ . \tag{181}$$

We can combine the information in these two equations into a generalized eigenvalue problem, in essence returning to the dimensionality of the original Hamiltonian.

$$\begin{pmatrix} (\underline{\tilde{H}}^{(o)} - ik\underline{L}^{(o)}) & \underline{V}^{(oc)} \\ \underline{V}^{(co)} & \underline{\tilde{H}}^{(c)} \end{pmatrix} \begin{pmatrix} \bar{c}^{(o)} \\ \bar{c}^{(c)} \end{pmatrix} = k^2 \begin{pmatrix} \underline{Y}^{(o)} & \underline{0} \\ \underline{0} & \underline{Y}^{(c)} \end{pmatrix} \begin{pmatrix} \bar{c}^{(o)} \\ \bar{c}^{(c)} \end{pmatrix} \ . \tag{182}$$

We could diagonalize this equation as it stands, were it not for the presence of the eigenvalue, k, in front of the surface term in the matrix on the left. This feature of the problem arises from the application of the Siegert boundary condition. It is this feature that makes the problem more challenging, but it is also this feature of the problem that defines Siegert pseudostates and imbues them with their properties. We can double the dimension of the space of the problem in a manner analogous to the one-channel derivation (Sec. III A). We define

$$\bar{d}^{(o)} = ik\bar{c}^{(o)} \ , \tag{183}$$

and

$$\bar{d}^{(c)} = ik\bar{c}^{(c)} \ . \tag{184}$$

The information in Eqs. (182)-(184) can be captured as

$$\begin{pmatrix} -\underline{\tilde{H}}^{(o)} & -\underline{V}^{(oc)} & \underline{0} & \underline{0} \\ -\underline{V}^{(co)} & -\underline{\tilde{H}}^{(c)} & \underline{0} & \underline{0} \\ \underline{0} & \underline{0} & \underline{Y}^{(o)} & \underline{0} \\ \underline{0} & \underline{0} & \underline{0} & \underline{Y}^{(c)} \end{pmatrix} \begin{pmatrix} \bar{c}^{(o)} \\ \bar{c}^{(c)} \\ \bar{d}^{(o)} \\ \bar{d}^{(c)} \end{pmatrix} = ik \begin{pmatrix} -\underline{L}^{(o)} & \underline{0} & \underline{Y}^{(o)} & \underline{0} \\ \underline{0} & \underline{0} & \underline{0} & \underline{Y}^{(c)} \\ \underline{Y}^{(o)} & \underline{0} & \underline{0} & \underline{0} \\ \underline{0} & \underline{Y}^{(c)} & \underline{0} & \underline{0} \end{pmatrix} \begin{pmatrix} \bar{c}^{(o)} \\ \bar{c}^{(c)} \\ \bar{d}^{(o)} \\ \bar{d}^{(c)} \end{pmatrix} . \quad (185)$$

A minus sign has been multiplied throughout. With the definitions

$$\underline{\tilde{H}}_{II} = \begin{pmatrix} \underline{\tilde{H}}^{(o)} & \underline{V}^{(oc)} \\ \underline{V}^{(co)} & \underline{\tilde{H}}^{(c)} \end{pmatrix} , \quad (186)$$

$$\underline{Y}_{II} = \begin{pmatrix} \underline{Y}^{(o)} & \underline{0} \\ \underline{0} & \underline{Y}^{(c)} \end{pmatrix} , \quad (187)$$

$$\underline{L}_{II} = \begin{pmatrix} \underline{L}^{(o)} & \underline{0} \\ \underline{0} & \underline{0} \end{pmatrix} , \quad (188)$$

$$\bar{c}_{II} = \begin{pmatrix} \bar{c}^{(o)} \\ \bar{c}^{(c)} \end{pmatrix} , \quad (189)$$

$$\bar{d}_{II} = ik\bar{c}_{II} , \quad (190)$$

we can write the problem as

$$\begin{pmatrix} -\underline{\tilde{H}}_{II} & \underline{0} \\ \underline{0} & \underline{Y}_{II} \end{pmatrix} \begin{pmatrix} \bar{c}_{II} \\ \bar{d}_{II} \end{pmatrix} = ik \begin{pmatrix} -\underline{L}_{II} & \underline{Y}_{II} \\ \underline{Y}_{II} & \underline{0} \end{pmatrix} \begin{pmatrix} \bar{c}_{II} \\ \bar{d}_{II} \end{pmatrix} . \quad (191)$$

This generalized eigenvalue problem is identical to the result of the one-channel derivation. Siegert psuedostates are the basis that diagonalizes this matrix equation. It can be solved by $2(N+M)$ eigenpairs. Because this eigenvalue problem is identical to the eigenvalue problem explored in detail in Sec. III, its solutions will obey identical orthonormality (Eq. (58)) and completeness (Eqs. (62) and (81)) relations. We now have a very valuable and simple method of obtaining momentum—and therefore energy—eigenvalues and position-space eigenvectors of an arbitrary system of two coupled channels. We know the completeness and the orthonormality relations obeyed by the eigenvectors, and we therefore know how to expand a wave packet in the basis of these eigenvectors. We also know how this wave packet will develop in time.

One thing we would like to do with this formalism is calculate Feshbach resonances. In the next subsection, we discuss Feshbach resonances in general before we consider a specific coupled-well model. We obtain an analytic formula for the poles of the S-matrix, which correspond to bound states and Feshbach resonances. We diagonalize Eq. (191) to obtain an energy spectrum, and compare the states that appear to be Feshbach resonances to the spectrum of Feshbach resonances calculated analytically.

E. Feshbach resonance

Feshbach resonance is a multi-channel phenomenon. Like a shape resonance (Sec. III C), a Feshbach resonance is a positive-energy state with bound-state like properties. In multiple-channel interactions, one channel will define the zero of the energy scale. The other channels are then shifted up by various amounts (see Figs. 12 and 14). As was discussed in Secs. IV B and IV C, a particle's wave function will have components in several channels. If the kinetic energy of the particle is positive relative to the zero defined by the lowest-energy channel, it still may be below the asymptotic values of some of the other channels. As was discussed in Sec. IV D, these channels are closed. The particle will behave as if it is bound in these closed channels. However, the closed channels are coupled to the open channel, so the particle can still leak to infinity very quickly. There are particular energies where, rather than escaping through the open channel(s), the particle resonates in a quasibound state, essentially behaving as if bound in one of the closed channels. These particular energies can correspond to energies where true bound states would be present in the channel if the channel were isolated. Just as in the case of shape resonance, one can identify the energy of a Feshbach resonance by a peak in the scattering cross section. One can also determine the quasibound state's mean lifetime by the imaginary part of the state's complex energy. For more on the phenomenon of Feshbach resonance and multi-channel resonance see Refs. [1] and [2].

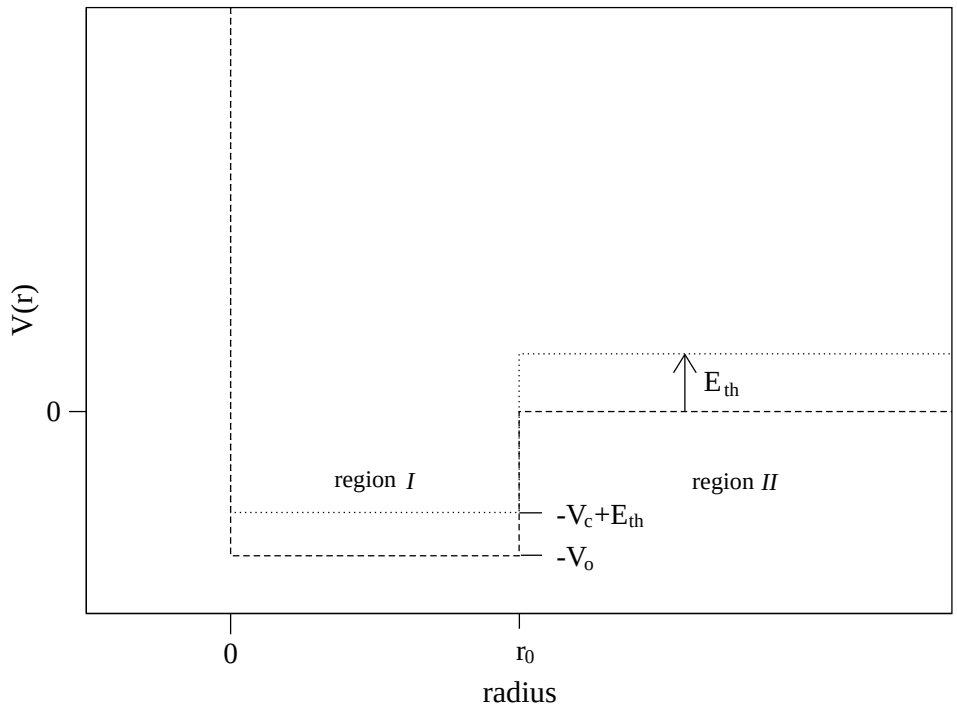

FIG. 14: The two-channel coupled square well model.

F. Analytical representation of the S-matrix in a coupled square well model

We consider coupled potential wells with a Hamiltonian of the form of Eq. (168). The potentials are given by

$$\hat{V}_o(r) = -V_o\Theta(r_0 - r) \ , \tag{192}$$

and

$$\hat{V}_c(r) = -V_c\Theta(r_0 - r) + E_{th} \ . \tag{193}$$

The coupling is constant for $r < r_0$ and zero beyond;

$$\hat{V}_{oc} = \hat{V}_{co} = V_{coup}\Theta(r_0 - r) \ . \tag{194}$$

The coupled wells are shown in Fig. 14. Notice that the well in the open channel defines the zero of the potential energy scale, and the closed-channel is shifted up by a threshold energy, E_{th}.

We develop this two-channel model analytically with the intention of testing the two-channel Siegert pseudostate formalism. Our goal is to obtain an expression for the poles of the scattering matrix. The outline of our strategy for solving this problem is as follows. We first obtain the eigensolutions in region I. Just as in the case of the coupled oscillators, they

will be sines. Here the derivatives (due to the kinetic energy operator in the Hamiltonian) are with respect to space, so the sines will oscillate in space rather than in time. We will then move back to the solutions of physical interest with a linear transformation. To find the full solutions, we will match the region I solutions to solutions in region II which have a known form due to the fact that they represent particles in the presence of channels of constant potential energy. The forms will be identical to the one channel case: in the open channel we will have superposed outgoing and incoming waves, and in the closed channel we will have the exponential decay of a bound state. We will match the region I solutions to the region II solutions with the same continuity conditions exercised in the one channel derivation—namely, the region I function and derivative values must match the region II function and derivative values at the discontinuity. The S-matrix element will appear as the ratio of outgoing to incoming wave amplitude in the open channel component of the region II solution. Algebraic manipulation of the equations resulting from enforcing the continuity conditions will provide us with an energy-dependent expression for S-matrix elements. Inspection of the matrix elements will reveal poles in the complex energy plane. For other treatments of this model, see Refs. [19] and [20].

First, we aim to find solutions obeying vanishing at the origin. We consider region I. We can separate the Schrödinger equation into the r-dependent kinetic energy operator, and the remaining r-independent components. The matrix of r-independent elements in region I is

$$\underline{W} = \begin{pmatrix} V_o + E & -V_{oc} \\ -V_{oc} & V_c + E - E_{th} \end{pmatrix} . \tag{195}$$

The r-dependent kinetic energy operator can be written in matrix form as

$$\underline{d}_r^2 = \begin{pmatrix} \frac{1}{2}\frac{d^2}{dr^2} & 0 \\ 0 & \frac{1}{2}\frac{d^2}{dr^2} \end{pmatrix} . \tag{196}$$

Because the r-dependent kinetic energy matrix is already diagonal, diagonalization of $\underline{W}$ is all that is required to obtain solutions in region I. The matrix whose columns are the eigenvectors of $\underline{W}$ we will call $\underline{A}$, and the diagonal matrix of eigenvalues of $\underline{W}$ we will call $\underline{\omega}^2$. Note that energy dependence is contained in $\underline{\omega}^2$, while $\underline{A}$ is energy-independent, just as in the case of the classical coupled oscillators. Again, we arrive at a matrix equation awaiting diagonalization, this time a standard eigenvalue problem. We diagonalize it in a

manner similar to the example of the coupled oscillators. We can write

$$\underline{WA} = \underline{A\omega}^2 \ , \tag{197}$$

and acknowledge that

$$\underline{AA}^T = \underline{A}^T \underline{A} = \underline{\mathbb{1}} \ , \tag{198}$$

which gives

$$\underline{A}^T \underline{WA} = \underline{\omega}^2 \ . \tag{199}$$

This contains the r-dependent information, while the entire Schrödinger equation in region I in this notation reads

$$\underline{d}_r^2 \underline{\phi}^{(I)}(r) + \underline{W}\underline{\phi}^{(I)}(r) = 0 \ . \tag{200}$$

Notice that we have arranged the solutions into a matrix; $\phi^{(I)}(r)_{ij}$ is the ith channel component of the jth solution. The superscript (I) on the solution matrix indicates that the solutions apply to region I. The notation is analogous to the one-channel treatment. Working with Eq. (200), we write

$$\underline{d}_r^2 \underline{AA}^T \underline{\phi}^{(I)}(r) + \underline{WAA}^T \underline{\phi}^{(I)}(r) = 0 \ . \tag{201}$$

Then,

$$\underline{A}^T \underline{d}_r^2 \underline{AA}^T \underline{\phi}^{(I)}(r) + \underline{A}^T \underline{WAA}^T \underline{\phi}^{(I)}(r) = 0 \ . \tag{202}$$

Using Eqs. (197) and (198) and the fact that $\underline{A}$ commutes with the second derivative operator, we obtain two uncoupled single-channel equations in the eigenrepresentation. The matrix of solutions obeying the uncoupled equations is

$$\underline{U}^{(I)}(r) = \underline{A}^T \underline{\phi}^{(I)}(r) \ . \tag{203}$$

We can write Eq. (202) as

$$\underline{d}_r^2 \underline{U}^{(I)}(r) + \underline{\omega}^2 \underline{U}^{(I)}(r) = 0 \ . \tag{204}$$

We have effectively rotated our eigenvalue problem into a basis where the channels are not coupled, as was done in the case of the coupled oscillators of Sec. IV C. The result is the 2×2 matrix equation of Eq. (204), wherein the matrices are diagonal. The two equations held in Eq. (204) are

$$\frac{d^2}{dr^2} U_i(r) + \omega_i^2 U_i(r) = 0 \ , \tag{205}$$

where $i = 1, 2$, and ω_i^2 is the ith eigenvalue of $\underline{W}$. Acknowledging vanishing at the origin, we know the solution to Eq. (205).

$$U_i(r) \propto \sin(\omega_i r) \ . \tag{206}$$

We leave this as a proportionality because our objective is to obtain an expression for the poles of the S-matrix. The normalization constant is irrelevant to this purpose.

Notice that the coupled wells lead to similar mathematics as the coupled springs of Sec. IV C. The classical oscillators obey a system of coupled equations which can be derived from Newton's laws or minimum action principles, whereas a particle in the coupled wells obeys Schrödinger's equation, which is an eigenvalue equation. Still, we handle the coupling in exactly the same way: we diagonalize the matrix with off-diagonal coupling blocks so as to represent the problem in its eigenbasis. In the case of the coupled oscillators, this provides us with the eigenmodes of oscillation and associated eigenfrequencies. In the coupled wells, we obtain identical information in the matrices $\underline{\omega}^2$ and $\underline{A}$. In this case, we have taken the derivation one step further and solved the resulting uncoupled differential equations to obtain $\underline{U}(r)$. In the case of the oscillators, this information was also accessible. We were dealing with a differential equation that was second order in time, so its solutions would have been given by Eq. (206), but with time as the independent variable. However, we must not lose sight of the fact that the information in these two contexts has a different physical interpretation. In the classical case, solutions point to the position of a particle in time. In the quantum case, solutions give the probability of a particle being at a particular position. Though the math looks very similar, the physical interpretation is remarkably different.

With the eigensolutions $U_i(r)$ known, we can move back to the coupled-channel solutions with

$$\underline{\phi}^{(I)}(r) = \underline{A}\underline{U}^{(I)}(r) \ . \tag{207}$$

Our next task is to match these solutions, which are valid in region I, to solutions in region II with the appropriate continuity conditions. In the open channel, we will get scattering behavior—the superposition of an incoming and an outgoing wave. In the closed channel, the wave will evanesce. Because the physical solution outside will be a superposition of open and closed channel solutions, we write the physical solution for $r > r_0$ as a column vector, anticipating that we will multiply the matrix of solutions in region I ($\underline{\phi}(r)$) by a vector of coefficients ($\bar{z}$) which will superpose the coupled-channel solutions when we match at the

discontinuity.

$$\bar{\phi}^{(II)}(r) = \begin{pmatrix} Se^{ik^{(II)}r} - e^{-ik^{(II)}r} \\ Ne^{-q^{(II)}r} \end{pmatrix} ; \tag{208}$$

$$k^{(II)} = \sqrt{2E} ; \tag{209}$$

$$q^{(II)} = \sqrt{2(E_{th} - E)} . \tag{210}$$

The superscript (II) refers to solutions in region II, not solutions in a particular channel. The use of k and q distinguishes between channels. In the one-channel square well, there was never an occasion to introduce q, because there was only one channel. Note that e^{-qr} must go to zero by $r = r_f$ based on our demand that one channel is closed. This is essentially the demand that $E < E_{th}$. Note that S in Eq. (208) is an element of the scattering matrix at energy E. It is this S that we seek. It contains the ratio of outgoing to incoming wave amplitude. Also, N is the closed-channel amplitude. We will not derive an expression for N in this study.

We aim to derive an expression for S by matching the region I solutions and derivatives to the region II solutions and derivatives, as was done in the one-channel case in Sec. III H. As mentioned above, our intuition tells us that we must superpose the open- and closed-channel region I solutions to match to the physical solution in region II. We accomplish this using

$$\bar{z} = \begin{pmatrix} z_1 \\ z_2 \end{pmatrix} . \tag{211}$$

For notational convenience, we also introduce

$$\bar{a}(r) = \begin{pmatrix} e^{ikr} \\ 0 \end{pmatrix} , \tag{212}$$

$$\bar{S} = \begin{pmatrix} S \\ N \end{pmatrix} , \tag{213}$$

and

$$\underline{b}(r) = \begin{pmatrix} e^{ikr} & 0 \\ 0 & e^{-qr} \end{pmatrix} . \tag{214}$$

We will now drop the superscript (I) associated with the matrix $\underline{U}$ for notational simplicity. The reader must remember that the eigensolutions in $\underline{U}$ are only valid in region I. The

equation resulting from the matching of function values at the discontinuity reads

$$\underline{AU}(r_0)\bar{z} = -\bar{a}(r_0) + \underline{b}(r_0)\bar{S} \; . \tag{215}$$

Matching derivatives at the discontinuity, we find

$$\underline{AU}'(r_0)\bar{z} = -\bar{a}'(r_0) + \underline{b}'(r_0)\bar{S} \; . \tag{216}$$

Because we seek an expression for S rather than the actual wave functions, we eliminate $\bar{z}$. After multiplying Eq. (215) from the left by $\underline{U}^{-1}(r_0)\underline{A}^T$, we arrive at

$$\bar{z} = -\underline{U}^{-1}(r_0)\underline{A}^T\bar{a}(r_0) + \underline{U}^{-1}(r_0)\underline{A}^T\underline{b}(r_0)\bar{S} \; . \tag{217}$$

Note that $\underline{U}^{-1}(r_0)$ is essentially a diagonal matrix with $1/\sin(\omega_i r_0)$ for a diagonal element. Inserting Eq. (217) into Eq. (216), we obtain

$$-\underline{AU}'(r_0)\underline{U}^{-1}(r_0)\underline{A}^T\bar{a}(r_0) + \underline{AU}'(r_0)\underline{U}^{-1}(r_0)\underline{A}^T\underline{b}(r_0)\bar{S} = -\bar{a}'(r_0) + \underline{b}'(r_0)\bar{S} \; . \tag{218}$$

The R-matrix, in this context given by

$$\underline{R} = \underline{XU}'(r_0)\underline{U}^{-1}\underline{X}^T \; , \tag{219}$$

is well known in scattering theory (see, for instance, Ref. [1]). We continue with our pursuit of the S-matrix element. Our equation reads

$$\underline{R}\bar{a}(r_0) - \underline{Rb}(r_0)\bar{S} = \bar{a}'(r_0) - \underline{b}'(r_0)\bar{S} \; , \tag{220}$$

which can be rearranged to give

$$\bar{S} = \left[-\underline{Rb}(r_0) + \underline{b}'(r_0)\right]^{-1}\left[-\underline{R}\bar{a}(r_0) + \bar{a}'(r_0)\right] \; , \tag{221}$$

or, more explicitly.

$$\begin{pmatrix} S \\ N \end{pmatrix} = \begin{pmatrix} (ik - R_{11})e^{ikr_0} & -R_{12}e^{-qr_0} \\ -R_{21}e^{ikr_0} & -(q + R_{22})e^{-qr_0} \end{pmatrix}^{-1} \begin{pmatrix} -(R_{11} + ik) \\ -R_{21} \end{pmatrix} \; . \tag{222}$$

The poles of the S-matrix occur at locations where the inverse of the matrix in Eq. (222) does not exist, that is, where

$$\det \begin{pmatrix} (ik - R_{11})e^{ikr_0} & -R_{12}e^{-qr_0} \\ -R_{21}e^{ikr_0} & -(q + R_{22})e^{-qr_0} \end{pmatrix} = 0 \; . \tag{223}$$

The formula satisfied at a pole of the S-matrix is then

$$(R_{11} - ik)(q + R_{22}) - R_{21}^2 = 0 \; . \tag{224}$$

This is the formula we have been seeking. k and q are functions of energy (Eqs. (209) and (210)), so this equation can be solved for a discrete spectrum of energy values corresponding to bound states and Feshbach resonances.

Having derived this formula, we can now test the two-channel Siegert pseudostate formalism. We will diagonalize Eq. (191) to obtain a k and E spectrum. We will then search for correspondence between certain values of E obtained by diagonalization of Eq. (191) and values of E for which Eq. (224) is satisfied. We expect that all negative values of energy obtained upon diagonalization of Eq. (191) will satisfy Eq. (224), whereas only select values of E in the positive ReE pseudocontinuum will satisfy Eq. (224). These will be the energies of Feshbach resonances. We must be careful not to give attention to energies for which decay of the form $e^{-\sqrt{2(E_{th}-E)}r}$ will not be sufficiently close to zero for $r = r_f$.

G. Feshbach resonances in a spectrum of Siegert pseudostates

We would now like to utilize our two-channel Siegert pseudostate formalism in calculating Feshbach resonances. We must establish its validity. Our method is as follows. We will diagonalize Eq. (191) to obtain an energy pseudocontinuum. We will observe behavior only in the low energy regime in consideration of the fact that we have declared one channel closed. We will then test energies to see if they are solutions to Eq. (224), that is, to see if they are poles of the S-matrix. This will lead to the identification of all of the low-energy Feshbach resonances present in our model. We will then demonstrate the ability to tune the energy of a Feshbach resonance by varying parameters of the model.

We begin by diagonalizing Eq. (191) in the presence of the coupled wells of Eqs. (192), (193) and (194) (Fig. 14), with the parameters $V_o = 5, V_c = 9, E_{th} = 6, V_{coup} = .1, r_0 = 8$, and $r_f = 24$. We obtain a complete k and energy spectrum. However, many of the higher-energy solutions are not valid due to the fact that we artificially forced them to zero at r_f. In Eq. (208), we write the closed-channel solution as $e^{-q^{(II)}r}$ where $q^{(II)} = \sqrt{2(E_{th} - E)}$. We only consider energies that give closed-channel wave functions which decay to zero by $r = r_f$. This low-energy portion of the spectrum is shown in Fig. 15. We see the bound and

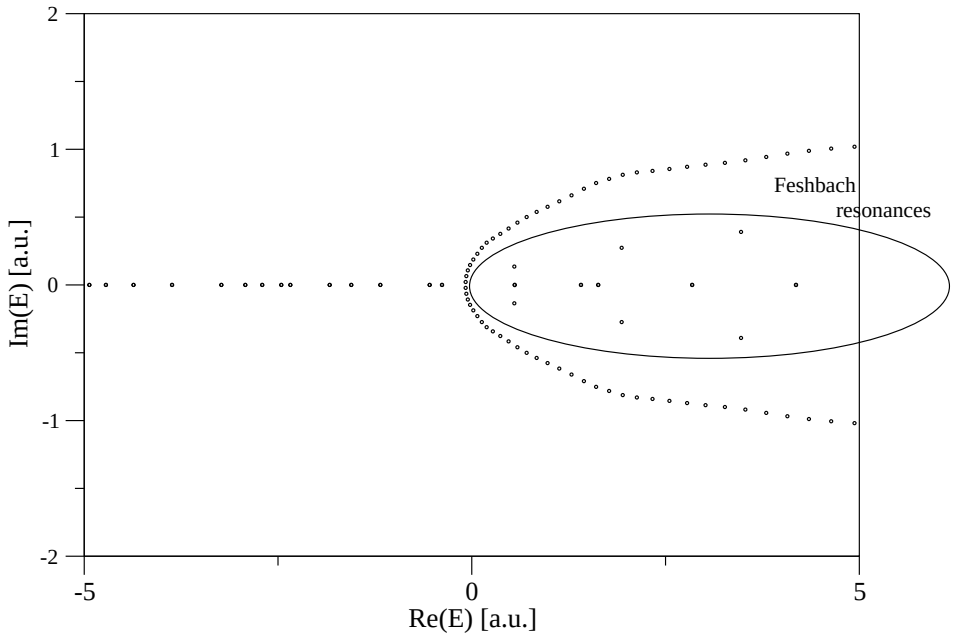

FIG. 15: The low-energy portion of the energy spectrum of the coupled square well model. The bound and antibound states lie on the negative real energy axis. The branches of the pseudocontinuum appear just as in Fig 4. Feshbach resonances are isolated from the pseudocontinuum. They are poles of the S-matrix, satisfying Eq. (224).

antibound states with negative energy, and we see the branches of the pseudocontinuum. There is a structure of states with smaller imaginary part of energy nested within the pseudocontinuum. These are the Feshbach resonances. They stand out from the rest of the energy spectrum in the same way shape resonances did in the one-channel case. We plug them into Eq. (224) and find that they all correspond to poles of the S-matrix, as do the bound and antibound states. The pseudocontinuum energies do not satisfy Eq. (224). This numerical test confirms the ability of two-channel Siegert pseudostates to capture Feshbach resonances.

H. Tuning Feshbach resonances

Now we would like to demonstrate our ability to tune a Feshbach resonance via the adjustment of an external parameter. Notice that the adjustment of E_{th} in the closed channel (See Eq. (193) and Fig. 14) moves the closed channel relative to the open channel. Such adjustment of the relative position of channels can be achieved by varying the magnitude of

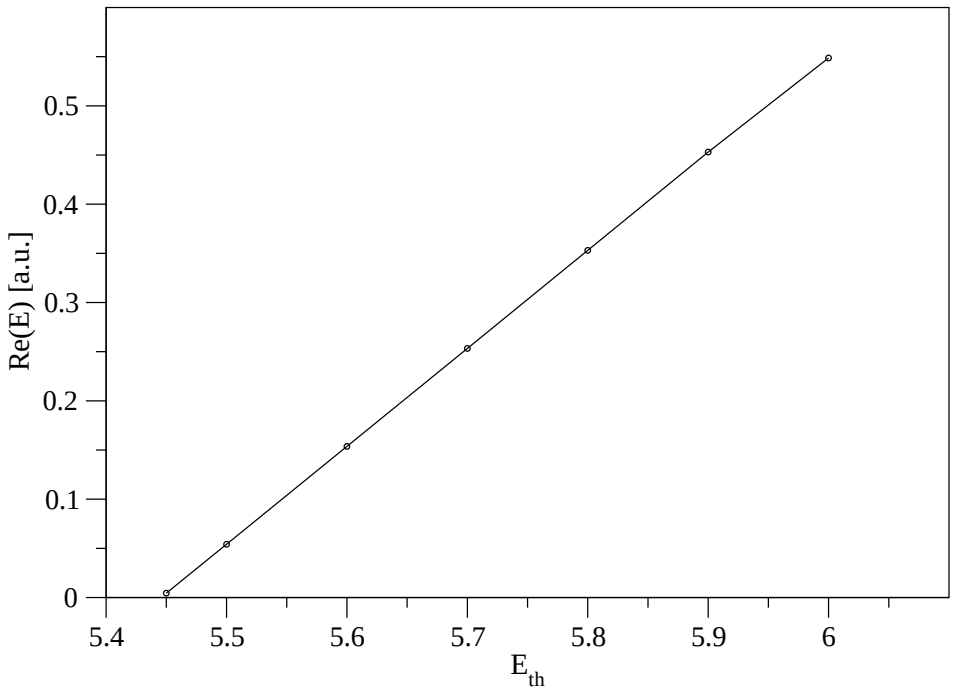

FIG. 16: The real part of the energy of a Feshbach resonance vs. the parameter E_{th}. The parameter E_{th} controls the position of the closed channel relative to the open channel. Notice the linear dependence of the energy of the Feshbach resonance on this parameter. E_{th} can signify a physical parameter, such as an external magnetic field. This plot demonstrates that one can vary the position of a Feshbach resonance by varying an external physical parameter.

an external parameter, such as a magnetic or electric field. We can think of changing the parameter E_{th}, which shifts the closed channel relative to the open channel, as being related to changing an experimental parameter, like the strength of an external field.

Suppose we then consider a gas of particles at a given temperature. We cannot control the kinetic energy of each individual particle in the gas, but we know the ensemble will have a distribution peaked around some average. If we are trying to form quasibound states, we would like to sweep the energy of a Feshbach resonance across the average kinetic energy of the particles in the ensemble. In order to demonstrate this ability, we simply follow the energy of a particular Feshbach resonance as we vary E_{th}. A plot of the real part of the energy of a Feshbach resonance versus E_{th} is shown in Fig. 16. It is clear that we are capable of tuning the position of a Feshbach resonance near threshold. The physics contained in this example are relevant to the creation of Bose-Einstein condensates, as well as fermionic condensates, where the quasibound states are related to Cooper pairs. Feshbach

resonances are also significant in subatomic particle collisions.

Calculating Feshbach resonances is one example of the utility of two-channel Siegert pseudostate theory. As was mentioned in the introduction, the most complete description of a scattering event is often contained in a time-dependent model. Siegert pseudostates are fully capable of serving as a basis for time-dependent scattering theory in two channels by employing the concepts of time evolution discussed in Sec. III to the two-channel SPS formalism. Studies of the physics of time evolution in multiple channel interactions will be saved for another time. Note, however, that if we would like to use Siegert pseudostates as a basis for cold collision theory, it is critical that we utilize the expression for time dependence of Eq. (108), which calls upon all $2N$ SPSs, because this representation proved much more accurate in the case of wave packets with low kinetic energy (see Table III).

V. CONCLUSIONS

A. General discussion of the findings

Through the window of Siegert pseudostates, this study has observed quantum-mechanical scattering in a basis of states associated with complex energies. In addition to representing all types of stationary states, including resonances in one and two channels, Siegert pseudostates (states with complex energies, obeying the Siegert boundary condition), have been seen to be capable of superposing into complete temporal illustrations of interaction events. In the introduction we discussed the challenges of scattering theory—to identify an entire spectrum of basis states, including bound states, continuum states, and resonances, to represent a physical state as a superposition of basis states, and to model the time evolution of the physical state. This study has demonstrated that Siegert pseudostates provide a basis capable of meeting these challenges of scattering theory. In addition, by the nature of the Siegert boundary condition, the continuum is discretized, rendering it easy to handle mathematically.

The utility of Siegert pseudostates in solving physical problems has already been recognized by the physics community (see Refs. [21],[22],[23]). Still, there are puzzles to be pondered.

B. Future directions

Many avenues of further study are present. The formalism of Siegert pseudostates is not capable of accurately treating long range potentials. Long range potentials are present in all types of ionization problems, so it would be valuable to expand the formalism—perhaps using perturbative techniques—to treat such scenarios.

Cold atoms are a hot item these days. Treating collisions like those present during the formation of condensates is feasible. The methods discussed in this paper are capable of calculating the energy of a Feshbach resonance and then representing a wave packet evolving in time with average energy at the level of the Feshbach resonance. This could offer valuable insight into the physics of ultracold interactions. Because the discussed form of non-exponential time evolution utilizing $2N$ Siegert pseudostates has demonstrated its ability to accurately represent slow wave packets, the treatment of cold collisions is accessible to this method.

Another relevant topic that was not addressed in this study is the nonexponential time dependence of decaying quantum mechanical states. We have seen that accurate time evolution can be achieved with the Faddeeva function. When one looks at the form of the Faddeeva function in the long-time limit, one sees that the quasibound states evolve with the standard exponential phase factor seen in Eq. (110), but also that there is a decaying component that goes as $t^{-3/2}$. Physics of this sort may play a significant role in quantum computing, and other areas where the goal is to establish long term, coherent wave functions.

APPENDIX A: FINITE ELEMENT BASIS

Our numerics were carried out in a finite element basis of fifth-order Hermite interpolating polynomials. A discussion of our these basis functions is held in [26]. A radial mesh of nodes was arranged evenly in space. There were three finite elements present at each node, one with a function value, but zero first and second derivative, one with a first derivative, but zero function value and second derivative, and one with vanishing function value and first derivative but finite curvature. These are referred to as zero-, one-, and two-type finite elements, respectively. All three types vanish at the $i-1$th and $i+1$th nodes. The basis functions are shown in Fig. 17. For our consideration, we enforced vanishing at the origin.

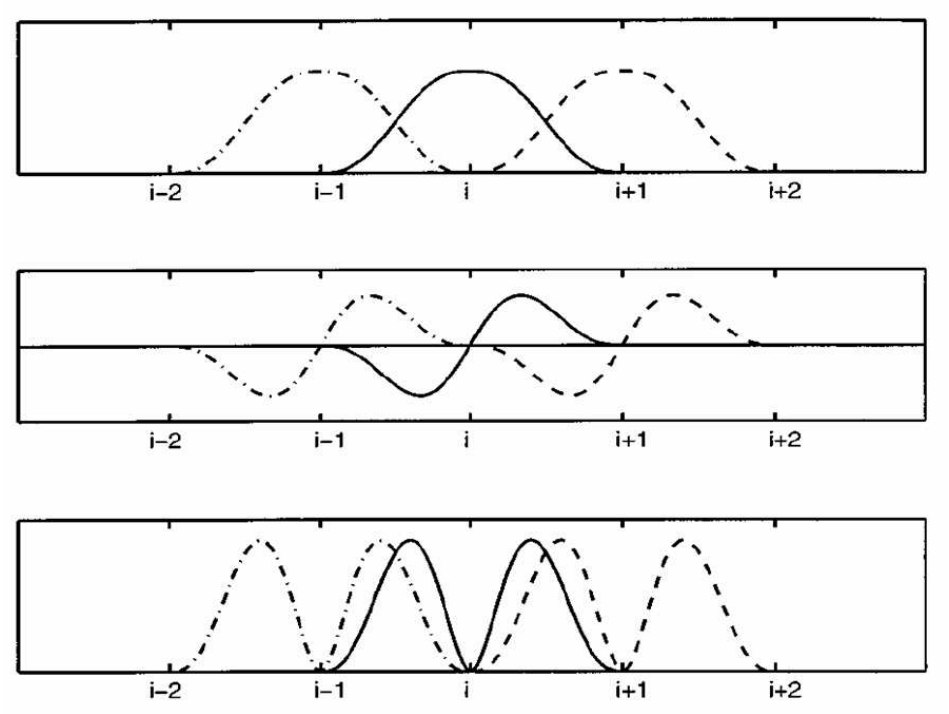

FIG. 17: The zero-, one-, and two-type finite element basis functions.

We only considered the one- and two-type polynomials at the first node.

APPENDIX B: CONTRASTING SPS THEORY WITH STANDARD QUANTUM MECHANICS

The mathematics associated with Siegert pseudostates strays from the conventions of quantum mechanics. Application of the Siegert boundary condition eliminates the Hermiticity of the Hamiltonian. It is generally accepted as a postulate of quantum mechanics that physical observables (of which energy is one) are represented by Hermitian operators which return real eigenvalues. We violated this postulate and found ourselves observing complex k and energy spectra. But this proved to be a useful aspect of the formalism. It was by analyzing these complex spectra that we were able to quickly identify resonances in one and two channels.

Further, restricting ourselves to consideration of solutions in a finite region of space and applying the Siegert boundary condition at the border led to a non-standard orthonormality

conditon. Siegert pseudostates obey

$$\int_0^{r_f} \varphi_m(r)\varphi_n(r)dr + i\frac{\varphi_m(r_f)\varphi_n(r_f)}{k_m + k_n} = \delta_{mn} \ , \tag{B1}$$

whereas eigensolutions to a standard Hermitian Hamiltonian obey

$$\int_0^{\infty} \phi_m^*(r)\phi_n(r)dr = \delta_{mn} \ . \tag{B2}$$

This seems like a minute difference, but Eq. (B1) does not actually qualify as an inner product. Because the vector space containing Siegert pseudostates does not have an inner product, it is not considered a Hilbert space. Therefore, the theory of Siegert pseudostates does not take place in Hilbert space. Another postulate of quantum mechanics says that the state of a particle at a given time is represented by a vector in a complex Hilbert space. But again, the digression from standard textbook quantum mechanics is beneficial. From our orthonormality condition (Eq. (B1)) we find the $\underline{M}$-matrix. Recall

$$\underline{M}_{mn} = \int_0^{r_f} \varphi_m(r)\varphi_n(r)dr = \delta_{mn} - i\frac{\varphi_m(r_f)\varphi_n(r_f)}{k_m + k_n} \ . \tag{B3}$$

Where this would be an identity matrix (if we conjugated one of the functions in the integrand), it now has many non-zero off-diagonal elements. And it was $\underline{M}$ that entered critically into our minimal completeness relation (Eq. (81)), which allowed us to represent an arbitrary wave packet with remarkable accuracy.

The postulate of quantum mechanics which concerns time evolution simply states that the vectors representing a state in a complex Hilbert space evolve in time according the time-dependent Schrödinger equation. As we have seen, Siegert pseudostates do not obey the time-dependent Schrödinger equation.

The formalism of Siegert pseudostates is simply one example where the theory of quantum mechanics makes use of more general mathematics than those present in complex Hilbert spaces. Complex energies have long been utilized in identifying resonances. Also, Liouville spaces are often utilized for many purposes related to quantum mechanics. That quantum mechanics can take place in Hilbert space is clear, but that quantum mechanics can also take place in other vector spaces is also the case.

[1] H. Friedrich, *Theoretical Atomic Physics* (Springer, Heidelberg, 1998).

[2] J. R. Taylor, *Scattering Theory* (Wiley, New York, 1973).

[3] R. Shankar, *Principles of Quantum Mechanics* (Plenum, New York, 1994).

[4] A. J. F. Siegert, Phys. Rev. **56**, 750 (1939).

[5] O. I. Tolstikhin, V. N. Ostrovsky, and H. Nakamura, Phys. Rev. A **58**, 2077 (1998).

[6] H. J. Korsch, R. Möhlenkamp, and H.-D. Meyer, J. Phys. B **17**,2955 (1984).

[7] R. G. Newton, *Scattering Theory of Waves and Particles* (Dover, Mineola, N.Y., 2002).

[8] R. M. More and E. Gerjuroy, Phys. Rev. A **7**, 1288 (1973).

[9] E. Anderson, Z. Bai, C. Bischof, S. Blackford, J. Demmel, J. Dongarra, J. Du Croz, A. Greenbaum, S. Hammarling, A. McKenney, and D. Sorensen, *LAPACK Users' Guide* (Society for Industrial and Applied Mathematics, Philadelphia, 1999).

[10] G. H. Golub and C. F. van Loan, *Matrix Computations* (Johns Hopkins, Baltimore, 1996).

[11] J. Blatt and V. F. Weisskopf, *Theoretical Nuclear Physics* (Dover, Mineola, 1991).

[12] R. Santra and L. S. Cederbaum, Phys. Rep. **368**, 1 (2002).

[13] R. Santra, J. M. Shainline, and C. H. Greene, Phys. Rev. A. **71**, 032703 (2005).

[14] The Faddeeva function in Eq. (110) was numerically evaluated using the algorithm described in Ref. [15].

[15] G. P. M. Poppe and C. M. J. Wijers, ACM Trans. Math. Software **16**, 38 (1990).

[16] V. N. Faddeeva and N. M. Terent'ev, *Tables of Values of the Function $w(z)$ for Complex Argument* (Pergamon, Oxford, 1961).

[17] M. L. Goldberger and K. M. Watson, *Collision Theory* (Wiley, New York, 1964).

[18] G. V. Sitnikov and O. I. Tolstikhin, Phys. Rev. A. **67**, 032714 (2003).

[19] S. J. J. M. F. Kokkelmans, J. N. Milstein, M. L. Chiofalo, R. Walser, and M. J. Holland, Phys. Rev. A **65** 053617 (2002).

[20] C. G. Meister and H. Friedrich, Phys. Rev. A **66** 042718 (2002).

[21] E. L. Hamilton and C. H. Greene, Phys. Rev. Lett. **89**, 263003 (2002).

[22] O. I. Tolstikhin, I. Y. Tolstikhina, and C. Namba, Phys. Rev. A **60**, 1050 (1999).

[23] K. Toyota and S. Watanabe, Phys. Rev. A **68** 062504 (2003).

[24] V. Kokoouline and C. H. Greene, Phys. Rev. A **69**, 032711 (2004).

[25] R. Santra, K. V. Christ, and C. H. Greene, Phys. Rev. A **69**, 042510 (2004).

[26] K. V. Christ, Undergraduate Honors Thesis, University of Colorado (2003).

[27] S. Yoshida, S. Watanabe, C. O. Reinhold, and J. Burgdörfer, Phys. Rev. A **60**, 1113 (1999).

[28] S. Tanabe, S. Watanabe, N. Sato, M. Matsuzawa, S. Yoshida, C. Reinhold, and J. Burgdörfer, Phys. Rev. A **63**, 052721 (2001).

[29] M. Abramowitz and I. A. Stegun (Eds.), *Handbook of Mathematical Functions* (Dover, New York, 1970).

[30] J. H. Kwak and S. Hong, *Linear Algebra* (Birkhäuser, Boston, 2004).

[31] S. T. Thornton and J. B. Marion *Classical Dynamics of Particles and Systems* (Thomson, United States, 2004).

[32] Although we use the word "analytical", Eq. (146) is represented numerically in the tests.